Study on the role of hypothalamic prostaglandins in the regulation of systemic glucose metabolism

（マウスの全身糖代謝調節における視床下部プロスタグランジンの役割に関する研究）

Ming Liang LEE

Contents

Abbreviations

2DG	2-deoxy-D-glucose
AA	Arachidonic acid
AAV	Adeno-associated-virus
AgRP	agouti-related peptide
ARC	Arcuate nucleus
BAT	Brown adipose tissue
COX	Cyclooxygenase
cPLA2	cytosolic phospholipase A2
cPLA2KD^{Sf1}	mice with knockdown of *pla2g4a* in Sf1-neurons
DAPI	4',6-diamidino-2-phenylindole
DIO	Diet induced obesity
dm	dorsomedial
EET	epoxyeicosatrienoic acid
EGP	Endogenous glucose production
ESI	electrospray ionization
FA	Fatty acid
GFP^{Sf1}	mice with GFP expression in Sf1-neurons
GIR	Glucose infusion rate
GR	gastrocnemius muscle
GSIS	glucose-induced insulin secretion
HETE	hydroxyeicosatetraenoic acid
HFD	High fat diet
i.c.v.	Intracerebroventricular
i.p.	Intraperitoneally
IMS	imaging mass spectrometry
LC-MS	liquid chromatography–mass spectrometry
MAFP	methyl arachidonyl fluorophosphonate
MALDI	matrix-assisted laser desorption/ionization
NPY	neuropeptide Y
OA	oleic acid
PA	palmitic acid
PE	phosphatidyl-ethanolamine
PI	phosphatidyl-inositol
PLC	Phospholipase C
POMC	Proopiomelanocortin
PS	phosphatidyl-serine
PUFA	polyunsaturated fatty acids
RCD	Regular chew diet
Rd	Ratio of disappearance
SA	stearic acid
sPLA2	secretory phospholipase A2
TIC	total ion current
TOF	time-of-flight
vl	ventrolateral
VMH	Ventromedial hypothalamus
WAT	white adipose tissue

Author's Declaration

This study is my original work in Graduate School of Veterinary, Hokkaido University. The contents of this study has not been presented at any other University for the award of a degree. A part of this thesis has been published as follow:

Lee ML, Matsunaga H, Sugiura Y, Hayasaka T, Yamamoto I, Ishimoto T, Imoto D, Suematsu M, Iijima N, Kimura K, Diano S, Toda C. Prostaglandin in the ventromedial hypothalamus regulates peripheral glucose metabolism. Nat Commun 12, 2330, 2021.

Introduction

Recent evidence from animal models indicates that the brain plays a critical role in the systemic regulation of glucose metabolism[1,2]. Neurons in the hypothalamus integrate hormonal and nutritional information and maintain glucose homeostasis by controlling metabolism in peripheral tissues. The role of hypothalamus on body condition has been observed at as early as 1940s[3]. In particular, the ventromedial nucleus of the hypothalamus (VMH) and arcuate nucleus of the hypothalamus (ARC) are critical nuclei for the glucose metabolism and body energy homeostasis. To regulate whole body energy homeostasis, there are specialized glucose-sensing neurons to detect ambient glucose in these regions: the glucose-excited (GE) neurons and the glucose-inhibited (GI) neurons, which are excited or inhibited by glucose, respectively. These glucose-sensing neurons each constitutes about 10 to 15 percent of all steroidogenic factor 1 (Sf1) neurons in the VMH[4]. The Sf1 neurons are the majority of neurons and constitute ~60% of total neurons in the dm/cVMH[5]. Activation of Sf1 neurons by optogenetics increases endogenous glucose production (EGP)[6] and simultaneously enhances insulin sensitivities in several tissues such as liver, muscle and brown adipose tissue (BAT)[7]. Hormones, including insulin, leptin and ghrelin, regulate glucose metabolism by changing the activities of these neurons and their gene expression. Insulin is the major peptide to increase blood glucose clearance by promoting glucose uptake of peripheral tissue and inhibiting gluconeogenesis. Insulin hyperpolarizes a subset of Sf1 neurons through PI3 kinase pathway[8]. Interestingly, although the insulin is considered to control blood glucose and insulin resistance is the main indicator of metabolic disorders, the insulin mediated-inhibition of Sf1 neurons is one of the factors to cause high-fat-diet induced obesity[9,10]. Leptin is another peptide to regulate food intake and energy homeostasis which secreted by adipose tissue[11]. Even though the leptin activates or inhibits different populations of Sf1 neurons, the effect of leptin on VMH increases glucose utilization and insulin sensitivity in peripheral tissues[8,12–14]. ARC is another core region to regulate energy homeostasis by regulating food intake and glucose metabolism[15]. There are two main neuronal populations in the ARC, the orexigenic agouti-related peptide (AgRP) neurons, which co-express neuropeptide Y (NPY), and the anorexigenic proopiomelanocortin (POMC) neurons[16]. POMC and AgRP neurons control EGP in opposite ways, i.e., activation of POMC increases insulin sensitivity in the liver, while AgRP activation decreases liver insulin sensitivity[17,18]. Besides, subpopulations of POMC and AgRP neurons are also GE neurons and GI neurons respectively[19].

Obesity attenuates the function of these nuclei and promotes type II diabetes via hypothalamic inflammation[20]. In line with this, the glucose sensitivity was decreased in GE neurons and augmented in GE neurons of VMH from HFD-induced obesity mice[21], suggesting HFD impaired neuronal glucose-sensing to disturb systemic glucose metabolism. However, the mechanism how HFD impairs these neurons and how initiates hypothalamic inflammation remain unclear.

Fatty acids regulate the activities of hypothalamic neurons[19] and the lipid metabolism within the hypothalamus plays important roles in energy balance and glucose metabolism[22,23]. Phospholipids with

biologically active polyunsaturated fatty acids (PUFAs), including phosphatidyl-inositol (PI), phosphatidyl-ethanolamine (PE) and phosphatidyl-serine (PS), are abundantly found in the brain[24]. Some membrane phospholipids generate free PUFAs to regulate physiological functions of the brain. For example, phospholipase A2 (PLA2) preferentially generates arachidonic acid (AA) from phospholipids[25]. AA plays roles in several physiological functions, including thermogenesis in BAT and increasing blood glucose levels[26]. AA is also the precursor for eicosanoids such as prostaglandin and hydroxyeicosatetraenoic acid (HETE). Other PUFA, such as oleic acid (OA), modulates activities of nutrient-sensing neurons to regulate insulin secretion[27], and intracerebroventricular injection of OA enhances insulin sensitivity in the liver[28]. However, the distributions of FAs, PUFAs and PUFA-containing phospholipids in the hypothalamus and their roles in whole-body glucose metabolism are not clearly understood.

Here, we explore hypothalamic lipid metabolism in the regulation of systemic glucose homeostasis and its potential role in the development of diabetes using imaging mass spectrometry (IMS). We found that glucose injection in mice fed on a regular chow diet induces a decrease in phospholipids containing AA, which is mediated by cytosolic phospholipase A2 (cPLA2). Prostaglandins produced by phospholipids in the hypothalamus activate VMH neurons and increases insulin sensitivity in skeletal muscles. However, hypothalamic cPLA2-mediated prostaglandin production is enhanced by high-fat-diet and induces neuroinflammation, and blockage of this enzyme confers resistance to developing diabetes.

Materials and methods

Animals

Sf1-cre mice were purchased from the Jackson Laboratory (STOCK Tg(Nr5a1-cre)7Lowl/J; Bar Harbor, ME). For IMS and assessing the effects of inhibitors, male C57BL6J mice were purchased from Charles River Laboratories Japan. All mice were kept at 22–24 °C with a 12-h light/12-h dark cycle and given *ad libitum* food access. Animal care and experimental procedures were performed with approval from the Animal Care and Use Committee of Hokkaido University.

Imaging mass spectrometry

Glucose (2 g/kg body weight, Sigma-Aldrich, St. Louis, MO) or saline were injected intraperitoneally (i.p.) and the mice were sacrificed 30 min after injection. Brains were collected and were immediately embedded in 2% sodium carboxymethyl cellulose solution and frozen with liquid nitrogen. The 10-μm brain sections were prepared by cryostat and immediately mounted onto an indium-tin-oxide-coated glass slide (Bruker Daltonics, Bremen, Germany). The sections on the glass slides were immediately dried and stored at −20 °C until imaging mass spectrometry analysis.

Brain slices were sprayed with 9-aminoacridine matrix (10 mg/mL in 70% ethanol, Sigma-Aldrich) and installed into a matrix-assisted laser desorption/ionization (MALDI)-time-of-flight (TOF)/TOF system using ultrafleXtreme (Bruker Daltonics). Brain sections were irradiated by a smart beam (Nd:YAG laser, 355-nm wavelength); with a 25-μm irradiation pitch. The laser had a repetition frequency of 2000 Hz and mass spectra were obtained in the range of *m/z* 200–1200 in negative-ion mode. The *m/z* values from previous reports were used to label each lipid and phospholipid (Table 1). All ion images were reconstructed with total ion current (TIC) normalization by flexImaging (Bruker Daltonics) and transferred to ImageJ after modifying the grayscale. The areas of the VMH were identified by DAPI staining in the other brain sections and the brightness of the VMH and ARC were calculated as intensity. The intensity ratio in glucose injected mice against saline mice were statistically compared using the Wilcoxon test.

Quantification of PGs

Glucose (2 g/kg body weight, Sigma-Aldrich) or saline were injected i.p. two times (t = 0 and t = 30 min) and mice were sacrificed at t = 60 min. A HFD (45 kcal% fat, D12451, Research Diet, NJ) was given for 8 weeks. Hypothalamus was collected and immediately frozen in liquid nitrogen. The tissue was homogenized with 500 μl of MeOH:formic acid (100:0.2) containing an internal standard consisting of a mixture of deuterium-labeled PGs using microtip sonication. The samples were submitted to solid phase extraction using an Oasis HLB cartridge (5 mg; Waters, Milford, MA) according to the method of Kita et al[29]. Briefly, samples were diluted with water:formic acid (100:0.03) to give a final MeOH concentration of ∼20% by volume, applied to preconditioned cartridges, and washed serially with water:formic acid (100:0.03), water:ethanol:formic acid (90:10:0.03), and petroleum ether. Samples were eluted with 200 μl of MeOH:formic acid (100:0.2). The filtrate was concentrated with a vacuum

concentrator (SpeedVac, Thermo Fisher Scientific, Waltham, MA). The concentrated filtrate was dissolved in 50 μL of methanol and used for liquid chromatography/mass spectrometry (LC-MS).
Hypothalamic PGs were quantified by modified LC-MS[30]. Briefly, a triple-quadrupole mass spectrometer equipped with an electrospray ionization (ESI) ion source (LCMS-8060; Shimadzu Corporation, Kyoto, Kyoto, Japan) was used in the positive and negative-ESI and multiple reaction monitoring modes.

Stereotaxic surgeries and AAV injection

Male C57BL6J mice were anesthetized with mixture of ketamine (100 mg/kg) and xylazine (10 mg/kg) and were put on a stereotaxic instrument (Narishige, Tokyo, Japan). Mice were implanted with cannulae for intracerebroventricular (i.c.v.) or intra-hypothalamic injection. The i.c.v. cannulae were implanted in the lateral ventricle in an anterior–posterior (AP) direction: −0.3 (0.3 mm posterior to the bregma), lateral (L): 1.0 (1.0 mm lateral to the bregma), dorsal–ventrol (DV): −2.5 (2.5 mm below the bregma on the surface of the skull). The double-cannulae for intrahypothalamic injection had a gap of 0.8 mm between the two cannulae and were implanted following the coordinates of the AP: −1.4, L: ± 0.4, DV: −5.6. Cannulae were secured on the skulls with cyanoacrylic glue and the exposed skulls were covered with dental cement. To knock down expression of *pla2g4a* in the VMH, 6- to 8-week-old Sf1-cre mice were injected in each side of the VMH with ~0.5 μL AAV8-DIO-shRNA (Vigene Biosciences, Rockville, MD) against *mpla2g4* bilaterally using the following coordinates: AP: −1.4, L: ± 0.4, DV: −5.7. Open wounds were sutured after viral injection. Mice were allowed to recover for 5–7 days before experiments were started.

Glucose and insulin tolerance tests

A glucose tolerance test was performed on *ad libitum* fed or fasted mice. The *ad libitum* fed mice were used for assessing the effects of inhibitors. The fasted mice were used for assessing the phenotype of mice with knockdown of *pla2g4a* in Sf1-neurons (cPLA2KD^{Sf1}). To assess the effects of inhibitors, methyl arachidonyl fluorophosphonate (MAFP; 20 μM, 300 nL in each side), indomethacin (140 μM, 300 nL in each side), or vehicle were injected into both sides of the hypothalamus through a double-cannula. Glucose solution was then injected i.p. (2 g/kg) 30 min after intrahypothalamic injection. To assess the phenotype of cPLA2KD^{Sf1} mice, animals were fasted for 16 hours and injected with glucose (2 g/kg) i.p.. Blood glucose levels were measured by a handheld glucose meter (Nipro Free style, Nipro, Osaka, Japan) before injecting inhibitors (−30 min) or glucose (0 min), and measured at 15, 30, 60 and 120 min after glucose injection.
An insulin tolerance test was performed in *ad libitum* fed mice. The mice were i.p. injected with 0.5 U/kg insulin (Novo Nordisk, Bagsværd, Denmark). Blood glucose was measured before injecting inhibitors (−30 min) and glucose (0 min), and measured 15, 30, 60 and 120 min after glucose injection.

Serum insulin measurement

Mice were injected with inhibitors or vehicle into the hypothalamus using the same protocol as above. Blood from the tails was taken 30 min after intrahypothalamic injection. Then, glucose (2 g/kg) was i.p. injected and blood was taken at 15 and 30 min after glucose injection. The serums were collected after centrifuging for 10 min at 1000 ×g and maintained at −80°C until insulin was measured. The insulin concentration was measured with a Mouse Insulin ELISA KIT (FUJIFILM Wako, Osaka, Japan) and all procedures were followed by the protocols provided in the kit.

Real time PCR

Total RNA was extracted from the whole hypothalamus using Trizol solution (Invitrogen). *Pla2g4*, *Rbfox3* and *Actb* mRNA levels in the hypothalamus were measured by real-time TaqMan PCR. A high capacity cDNA reverse transcription kit (Thermo Fisher Scientific) was used for the reverse transcription. Real-time PCR (LightCycler 480; Roche) was performed with diluted cDNAs in a 20-μl reaction volume in triplicate.

Immunohistochemistry

Ad libitum fed mice were i.p. injected with either saline or glucose (3 g/kg) and perfused with heparinized saline followed by 4% paraformaldehyde (PFA) transcardially at 30 min after injection. Inhibitors were i.c.v. injected 30 min before glucose injection. Brain sections (50 μm each) containing the whole VMH were collected. Floating sections were incubated with rabbit-anti-cFos antibody (1:200, Santa Cruz Biotechnology, Denton, TX) or rabbit-anti-GFP antibody (1:1000, Frontier Institute, Hokkaido, Japan) in staining solution (0.1 M phosphate buffer (PB) containing 4% normal guinea pig serum, 0.1% glycine, and 0.2% Triton X-100) overnight at room temperature. To assess the cell population of astrocytes and microglia, sections were incubated with rabbit-anti-Iba1 antibody (1:3000, FUJIFILM Wako) or rabbit-anti-GFAP antibody (1:3000, Sigma-Aldrich) in staining solution overnight at room temperature. After rinsing with PB, sections were incubated in secondary antibody (1:500, Alexa Fluor 647 or 488 Goat Anti-Rabbit (IgG) secondary antibody, Cell Signaling Technologies, Danvers, MA) for 2 h at room temperature. The stained sections were washed with PB three times and mounted on glass slides with vectashield (Vector Laboratories, Burlingame, CA).

Assessment of phospholipase-A2 activity

Mice fed *ad libitum* were i.p. injected with either glucose (2 g/kg) or saline. Mouse hypothalami were collected 30 min after injection and stored at −80 °C until use. Tissues were homogenized and centrifuged at 10,000 ×g for 15 min at 4 °C and supernatants were collected. Activity of cytosolic- or secretory-phospholipase-A2 were measured following procedures described in the kit manuals (Abcam, Cambridge, UK).

Implantation of artery and vein catheter for clamp studies

Mice were anesthetized with pre-mixed ketamine (100 mg/kg) and xylazine (10 mg/kg). Polyethylene catheters were implanted into right carotid arteries and jugular veins. The tubes entered subcutaneously and protruded from the neck skin. Mice were allowed to recover for 3 to 5 days and tubes were flushed with heparinized saline each day.

Hyperinsulinemic–euglycemic clamp and measurement of 2[^{14}C] deoxy-D-glucose (2DG) uptake

The hyperinsulinemic–euglycemic clamp protocol was followed as described in previous papers[4,31]. The mice were fasted for 4 h and experiments were initiated in a free moving condition.

A 115-min clamp period (t = 0–115 min) was following a 90-min basal period (t = −90 to 0 min). A bolus of [3-^{3}H] glucose (5 mCi;) was injected through the jugular vein at the beginning of the basal period (t = −90 min) and tracer was infused at a rate of 0.05 mCi for 90 min. Blood samples were collected at t = −15 and −5 min to measure the rate of appearance (Ra). The clamp period was initiated with continuous infusion of insulin (2.5 mU/kg/min). During the clamp period, blood was collected, and blood glucose levels were measured from arterial blood every 5–10 min. Cold glucose was infused at a variable rate via the jugular vein catheter to maintain a blood glucose level at 110–130 mg/dL. Erythrocytes in withdrawn blood were suspended in sterile saline and returned to each animal.

To assess 2DG uptake, 2-[^{14}C] DG (10 mCi) was infused at t = 70 min and blood samples were collected at t = 75, 85, 95, 105, and 115 min. After collecting the blood sample at t = 115 min, mice were euthanatized, and small pieces of tissue samples from the soleus, Gastro-R (red portion of gastrocnemius), Gastro-W (white portion of gastrocnemius), BAT, heart, spleen, EWAT (epididymal white adipose tissue), brain (cortex), and liver were rapidly collected. The rate of disappearance (Rd), which reflects whole-body glucose utilization, rate of appearance (Ra), which mainly reflects endogenous glucose production (EGP), and the rates of whole-body glycolysis and glycogen synthesis were determined as described previously[31].

Statistical Analysis

Two-way or one-way ANOVA were used to determine the effect of inhibitors or knockdown of cPLA2 with the Prism 8 software (GraphPad). For repeated-measures analysis, ANOVA was used when values over different times were analyzed, followed by the Bonferroni and Sidak multiple comparisons tests. When only two groups were analyzed, statistical significance was determined by the unpaired Student's t test. A value of $p<0.05$ was considered statistically significant. All data are shown as mean ± SEM.

Results

Hyperglycemia decreases phospholipids and produces prostaglandins in the hypothalamus

To determine the distribution of FAs and phospholipids, hypothalamic slices were examined by IMS (Figure 1). The signal intensities of palmitic acid (PA), stearic acid (SA), AA and docosahexaenoic acid (DHA) were high around the third ventricle and the ventro-lateral region of the hypothalamus in C57BL/6J mice (Figure 1a). Similar distributions of phospholipids, such as phosphatidyl-ethanolamine (PE) (18:0/20:4), phosphatidyl-inositol (PI) (18:0/20:4) and PI (18:1/20:4) were also observed. However, signal intensities for phosphatidyl-serine (PS) (18:0/20:4) were low around the third ventricle while PS (18:0/22:6) distribution was ubiquitously observed (Figure 1b). We then measured hypothalamic lipids in mice that received an intraperitoneal (i.p.) glucose injection. Signal intensities for PI (18:0/20:4), PI (18:1/20:4) and PE (18:0/20:4) were significantly decreased in the VMH after glucose administration (Figure 1c and 1d). Similarly, the signal intensities for PI (18:0/20:4), PI (18:1/20:4), PE (18:0/20:4) and PS (18:0/16:0) were decreased in the ARC after glucose injection (Figure 1c and 1E). Hydrolysis of these phospholipids generates FAs, including AA (20:4), oleic acid (OA) (18:1), PA (16:0) or SA (18:0). However, the signal intensities of the four fatty acids were not changed after glucose injection, neither in the VMH nor ARC (Figure 1f to 1h).

AA is the source of eicosanoids and AA metabolism is catalyzed by enzymes such as cyclooxygenase (COX), lipoxygenase and cytochrome P450. To elucidate if glucose injection increased AA metabolism, we examined the effect of glucose injection on eicosanoid production in the whole hypothalamus using a liquid chromatography–mass spectrometry (LC-MS). Compared with saline, glucose injection increased COX-mediated hypothalamic production of prostaglandins, including 6-keto-PGF1α, PGD2, 13,14-dihydro-15-keto-PGF2α and PGE2 (Figure 1i to 1m). Lipoxygenase-mediated production of 12-HETE was increased in glucose-injected mice (Figure 2a). However, most of the lipoxygenase- and cytochrome P450-mediated production of HETEs and EETs was not detected or changed by glucose injection (Figure 2a and 2b). Thus, the data suggest that increased glucose levels decrease AA-containing phospholipids to produce prostaglandins.

Blocking the PLA2-mediated pathway in the hypothalamus impairs systemic glucose metabolism

PLA2 is the primary enzyme that generates AA from phospholipids[32] We then investigated the role of PLA2-mediated phospholipid utilization in glucose metabolism during acute hyperglycemia after an intrahypothalamic administration of methyl arachidonyl fluorophosphonate (MAFP), a PLA2 inhibitor. MAFP-injected mice showed decreased glucose tolerance compared to vehicle-injected mice and no changes in circulating insulin levels were observed (Figure 3a and 3b). Hypothalamic injection of indomethacin, an inhibitor of COX1/2, also impaired glucose tolerance, suggesting that prostaglandins regulate hypothalamic function to decrease blood glucose levels (Figure 3c and 3d). However, intra-hypothalamic injection of phospholipase C (PLC) inhibitor, U73122, or IP3 receptor antagonist, xestospondin 2, did not affect glucose tolerance (Figure 4). Thus, our results suggest that the PLA2-

mediated AA release and production of prostaglandins by COX1/2 in the hypothalamus, but not PLC-IP3 pathway, play a role in regulating glucose metabolism during acute hyperglycemia.

PLA2-mediated production of prostaglandin is necessary for the responsiveness of the VMH to glucose

To understand the role of PLA2 in controlling glucose metabolism, we examined the effect of PLA2 inhibitors on hypothalamic neuronal activation by cFos expression. Vehicle, MAFP or indomethacin were injected intracerebroventricularly (i.c.v.) 30 minutes prior to i.p. injection of either saline or glucose in fasted mice. In i.c.v. vehicle-injected mice, glucose administration increased cFos-positive cells in the dorsomedial (dm) and ventrolateral (vl) regions of the VMH and in the ARC (Figure 3e to 3g). In i.c.v. MAFP-injected mice, glucose did not alter the number of cFos-positive neurons in the dmVMH (Figure 3f). An increase in cFos-positive neurons after glucose injection was still detected in the vlVMH and ARC compared with saline injected mice (Figure 3f and 3g). Similar results were observed in i.c.v. indomethacin-injected mice after an i.p. injection of glucose (Figure 3f and 3g). Taken together, these data showing that both MAFP and indomethacin block neuronal activation during acute hyperglycemia in the dmVMH, indicating that metabolites of phospholipid-derived prostaglandins regulate glucose responsiveness of neurons in the dmVMH, while glucose activates neurons in the vlVMH and ARC independently of PLA2 and COX1/2.

Knockdown of *pla2g4a* in Sf1 neurons impairs glucose metabolism in regular chow diet feeding

Next, to explore the role of PLA2 in VMH neurons, short hairpin RNA (shRNA) against *pla2g4a*, a gene encoding cytosolic PLA2 (cPLA2), which has specificity for *sn*-2 arachidonic acid and a role in eicosanoid production [25], was transfected to the VMH through an adeno-associated virus (AAV) cre-recombinase (cre)-dependent in Sf1-cre mice (Figure 5a and 5b). Expression of *pla2g4a* mRNA was significantly decreased in the VMH of Sf1-cre mice injected with AAV-DIO-shRNA (cPLA2KD^{Sf1}) compared with AAV-DIO-GFP (GFP^{Sf1})-injected mice (Figure 5c). Although knockdown of *pla2g4a* did not influence body weight or the weight of adipose tissues, muscle and liver (Figure 5d), cPLA2KD^{Sf1} mice displayed decreased glucose tolerance and insulin sensitivity compared with GFP^{Sf1} mice (Figure 6a and 6b). To rule out the involvement of astrocytic cPLA2, AAV-GFAP-Cre and AAV-DIO-shRNA against *pla2g4a* were co-injected into the hypothalamus to knock down the expression of *pla2g4a* in hypothalamic astrocytes (Figure 7a and 7b). The knockdown of cPLA2 in astrocytes did not alter glucose metabolism, insulin sensitivity or body weight compared with control mice (Figure 7c to 7e). Thus, our data suggest that cPLA2 in Sf1 neurons, not astrocytes, regulates peripheral glucose metabolism.

To further investigate the role of cPLA2 in Sf1 neurons in glucose metabolism, we next performed hyperinsulinemic–euglycemic clamp studies. cPLA2KD^{Sf1} mice showed a lower glucose infusion rate (GIR) to maintain euglycemia compared with GFP^{Sf1} mice (Figure 6c to 3e). The rate of disappearance (Rd) and glycolysis were also lower in cPLA2KD^{Sf1} mice compared with GFP^{Sf1} mice (Figure 6f and

6g). However, endogenous glucose production (EGP) was not different between the two experimental groups (Figure 6h and 6i), suggesting that glucose utilization, rather than EGP, was impaired in cPLA2KD^{Sfl} mice. In agreement with this, cPLA2KD^{Sfl} mice showed decreased 2DG uptake in the red part of gastrocnemius muscle (GR) compared with control mice (Figure 6j). 2DG uptake in white adipose tissue (WAT) and the brain (cortex) were similar between groups (Figure 6k and 6l).

To assess changes in neuronal activation, we next analyzed cFos expression in cPLA2KD^{Sfl} mice compared with controls. Glucose-induced cFos expression in the dmVMH of cPLA2KD^{Sfl} mice was blunted compared with glucose-injected control mice (Figure 6m and 6n). The glucose-induced cFos expression in either vlVMH or ARC was not changed after the knockdown of cPLA2 (Figure 6m and 6o).

Taken together, our data suggest that cPLA2-mediated prostaglandin production regulates glucose-induced activation of dmVMH neurons to control insulin sensitivity in muscle.

High fat diet decreases AA-containing phospholipids and produces prostaglandins in the hypothalamus

High-fat-diet (HFD) induces inflammation and impairs hypothalamic functions[33]. Long chain fatty acyl CoA, a proinflammatory signal, accumulates in the hypothalamus during HFD feeding[34]. Thus, we examined the effect of HFD on lipid distribution in the hypothalamus. In mice fed an HFD for 8 weeks, the signal intensities for FAs, including AA, were greater in the ARC but not the VMH than those observed in control mice fed a RCD (Figure 8a to 8c). However, signal intensities for phospholipids in the hypothalamus were lower in HFD-fed mice (Figure 8d to 8f). In both the VMH and ARC, the signal intensities for PI (18:0/20:4), PI (18:1/20:4), PE (18:0/20:4), PE (p18:0/20:4) and PS (18:0/22:6) were significantly decreased in HFD-fed mice (Figure 8e and 8f). Because PLA2 generates AA from these phospholipids to regulate cellular activities, we next analyzed the activity of hypothalamic cPLA2 and found that cPLA2 activity was higher in HFD-fed mice compared with RCD-fed mice (Figure 8g). However, the activity of secretory phospholipase A2 (sPLA2) remained similar between RCD- and HFD-fed mice (Figure 8h).

We next explored the effect of HFD on the production of eicosanoids in the hypothalamus by LC-MS (Figure 8i and Figure 9). In HFD-fed mice, COX-mediated production of prostaglandins, including PGD2, PGF2α, PGE2, 11-beta-13,14-dihydro-15-keto-PGF2α, 13,14-dihydro-15-keto-PGD2 and 20-hydroxy-PGF2α, was increased compared with RCD-fed mice (Figure 8j to 8o). Only 12-HETE, an eicosanoid mediated by lipoxygenase, was significantly increased after HFD feeding (Figure 9).

Knockdown of *pla2g4a* improves HFD-induced impairment of glucose metabolism and recovers glucose responsiveness of the vlVMH and ARC to hyperglycemia.

To understand the role of HFD-induced activation of hypothalamic cPLA2, we fed cPLA2KD^{Sfl} mice with HFD and examined the role of cPLA2 on glucose metabolism. Body weight and tissue weight of HFD-fed cPLA2KD^{Sfl} mice (cPLA2KD^{Sfl}-HFD) were comparable to those of HFD-fed control

GFP^{Sf1} mice (GFP^{Sf1}-HFD) (Figure 10a and Figure 11). Unlike RCD-fed mice, knockdown of cPLA2 in Sf1 neurons increased glucose tolerance (Figure 10b). However, insulin tolerance test showed no difference between groups (Figure 10c). In GFP^{Sf1}-HFD mice, no significant changes in cFos-positive neurons in the VMH or ARC were observed after glucose injection compared with saline injection (Figure 10d to 10f). However, in cPLA2KD^{Sf1}-HFD, the number of cFos-positive neurons were significantly higher in the vlVMH and ARC after glucose injection compared with saline injection, suggesting that cPLA2 knockdown improved neuronal responsiveness to glucose (Figure 10d to 5f).

To understand the role of hypothalamic cPLA2 on glucose metabolism in HFD-fed mice, we performed hyperinsulinemic–euglycemic clamping (Figure 10g to 10m). To maintain euglycemia, GIR was significantly higher in cPLA2KD^{Sf1}-HFD than in GFP^{Sf1}-HFD (Figure 10g to 10i). Unlike RCD-fed mice, glucose utilization (Rd and glycolysis) in HFD-fed mice was not altered by knocking down cPLA2 (Figure 10j and 5k). In contrast, insulin inhibition of EGP was stronger during the clamp period in cPLA2KD^{Sf1}-HFD mice than in GFP^{Sf1}-HFD (Figure 10l and 5m). These results suggest that cPLA2 in the VMH has a deteriorative role in the glucose responsiveness of the vlVMH/ARC and attenuates hepatic insulin sensitivity during HFD-induced obesity. These data suggest that the role of cPLA2 and the mechanism to change glucose metabolism and neuronal activity by prostaglandins are different between HFD and RCD.

Knockdown of cPLA2 in Sf1 neurons prevents hypothalamic inflammation

We examined the effect of cPLA2 knockdown on hypothalamic inflammation, which attenuates neuronal functions, in HFD-fed mice. The mice were fed with a RCD or HFD for 8 weeks, and inflammation was measured by comparing the number of microglia and the astrocyte population. For this experiment, we used Iba1 and GFAP as markers of microglia and astrocytes, respectively (Figure 12). The number of Iba1 cells was increased in the ARC but not in the VMH after mice were fed with an HFD (Figure 12a to 12c). The numbers of Iba1 cells in the ARC, but not the VMH, were significantly decreased in a cPLA2KD^{Sf1}-HFD compared with a GFP^{Sf1}-HFD (Figure 12b and 12c). HFD also increased the number of GFAP cells in the ARC, but not in the VMH, compared with mice fed a RCD (Figure 12d to 12f). In the ARC, the number of GFAP-positive cells decreased in the cPLA2KD^{Sf1}-HFD mice compared with GFP^{Sf1}-HFD mice (Figure 12e and 12f), suggesting that cPLA2 in the VMH has an influence on inflammation in the ARC.

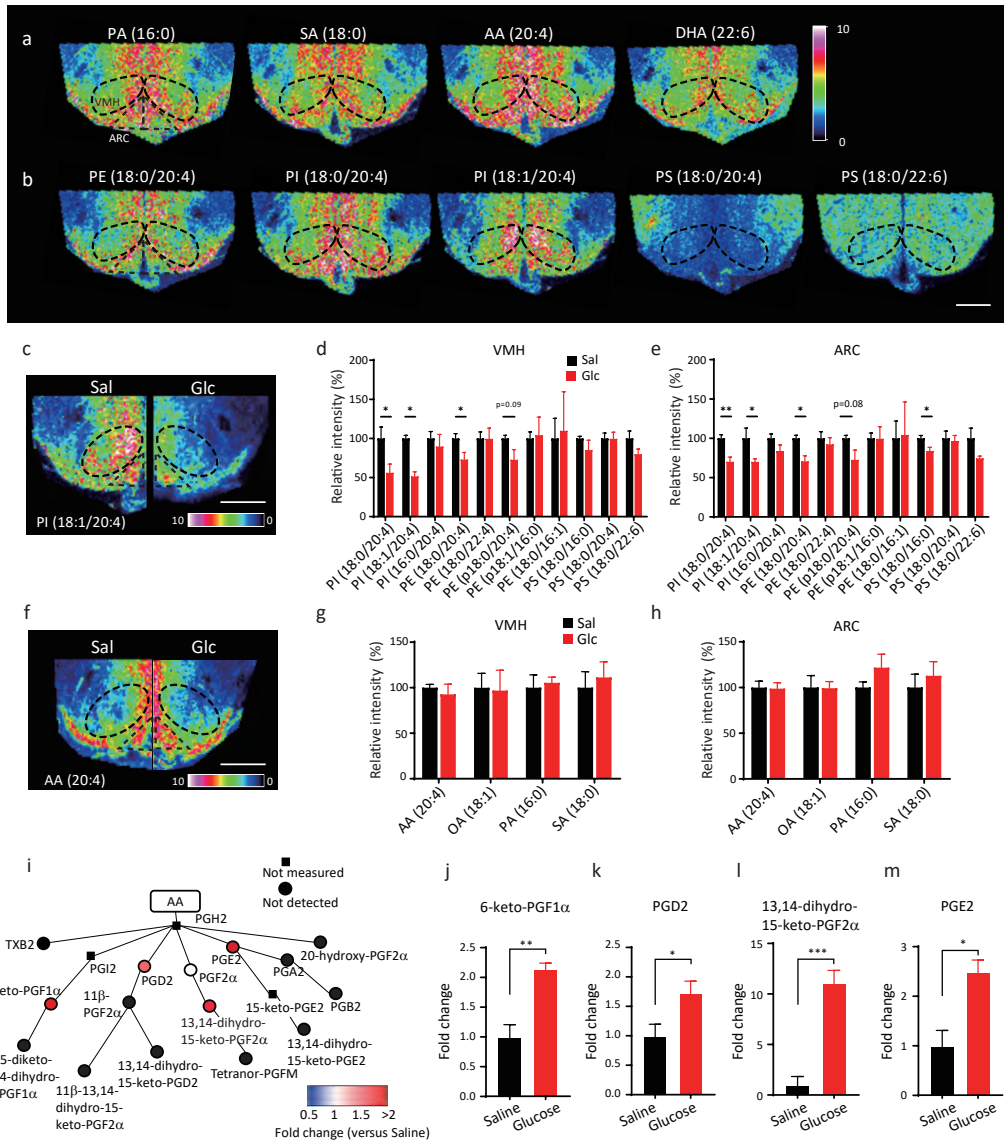

Figure 1. Hyperglycemia increases prostaglandin production derived from phospholipids. (a and b) Representative results of imaging mass spectrometry (IMS) showing distributions of hypothalamic fatty acids (a) and phospholipids (b) from untreated RCD-fed mice. The dashed black line shows the position of the VMH. Scale bar: 500 µm. (c to h) Distributions of phospholipids and fatty acids in the hypothalamus 30 min after injection of saline or glucose (2 g/kg). (c and f) Representative results of IMS on hypothalamic phosphatidylinositol (PI) (18:1/20:4) (c) and arachidonic acid (AA) (f) from mice i.p. injected with saline (left half) or glucose (right half). Scale bar: 500 µm. (d and e) Relative intensities of phospholipids in the VMH (d) and ARC (e) after injection with saline (n=5) or glucose (n=4). (g and h) Relative intensities of fatty acids in the VMH (g) and ARC (h) after injection with saline (n=5) or glucose (n=4). (i to m) LC-MS results showing the effects of glucose injection on AA metabolites in the whole hypothalamus. (i) Relative amounts of hypothalamic prostaglandins mediated by cyclooxygenase. (j) 6-keto-PGF1α, (k) PGD2, (l) 13,14-dihydro-15-keto-PGF2α and (m) PGE2 were increased by glucose injection. n=5 in each experimental group. (d) to (h) and (j) to (l) represent the mean ± SEM; * = $p<0.05$; ** = $p<0.01$; *** = $p<0.001$.

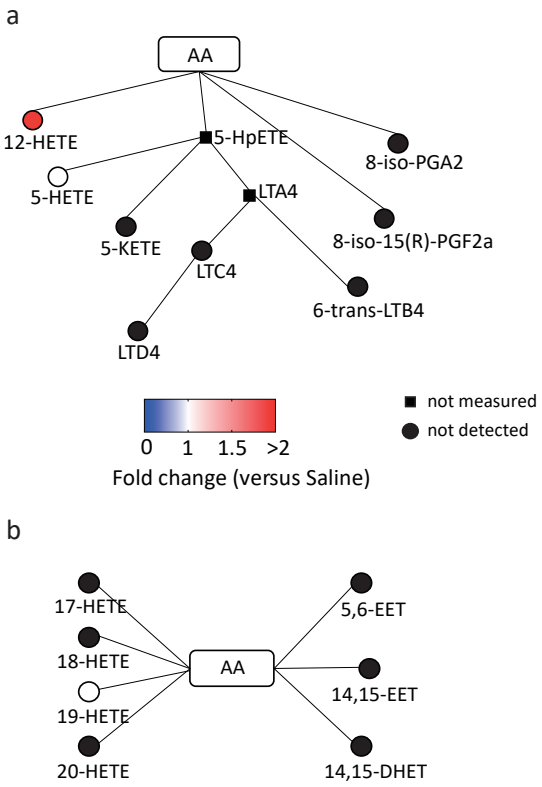

Figure 2. Effects of glucose on lipoxygenase or cytochrome P450 mediated eicosanoids in hypothalamus

Relative amounts of hypothalamic eicosanoids mediated by lipoxygenase (a) or cytochrome P450 (b) after the injection of glucose compared with saline injected mice. n=3 in each experimental group. Data represent the mean fold change in color.

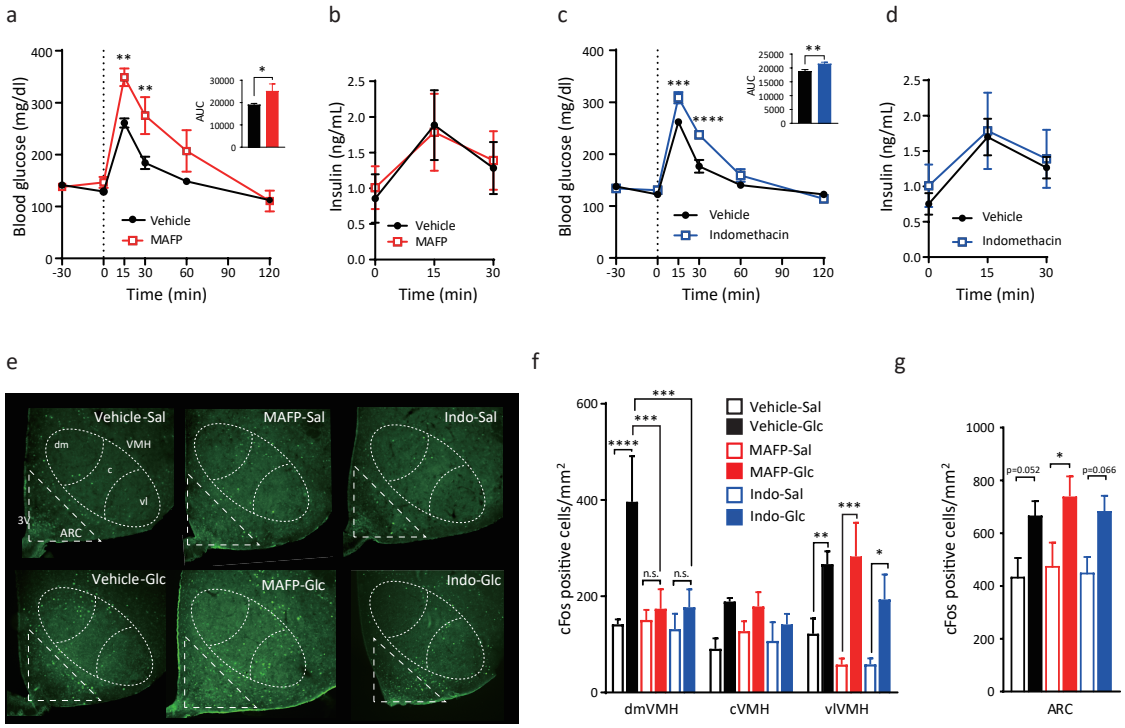

Figure 3. Hypothalamic PLA2- and COX-mediated AA metabolism regulates systemic glucose tolerance and modulates glucose responsiveness in the dmVMH.
(a) Glucose tolerance test (GTT) (0–120 min) after intra-hypothalamic injection (−30 min) of MAFP (n=7) or vehicle (n=7). (b) Blood insulin concentration of MAFP (n=7) or vehicle (n=7) injected mice during GTT. (c) GTT (0–120 min) after intra-hypothalamic injection (−30 min) of indomethacin (n=7) or vehicle (n=7). (d) Blood insulin concentration of indomethacin (n=7) or saline (n=7) injected mice during GTT. (e) Representative micrographs showing immunofluorescent cFos staining in the hypothalamus of saline (upper panels) or glucose (lower panels) injected mice after i.c.v. injection of PBS, MAFP or indomethacin (indo). Scale bar: 500 µm. dm: dorsomedial, c: central, vl: ventrolateral part of the VMH. (f and g) Quantification of cFos expression in the dorsomedial (dmVMH), central (cVMH) and ventrolateral (vlVMH) subregions of the VMH (f) and ARC (g) from mice injected with saline or glucose after i.c.v. injection of PBS, MAFP or indomethacin (n=3 in each experimental group). All data represent the mean ± SEM; * = p<0.05; ** = p<0.01; *** = p<0.001; **** = p<0.0001.

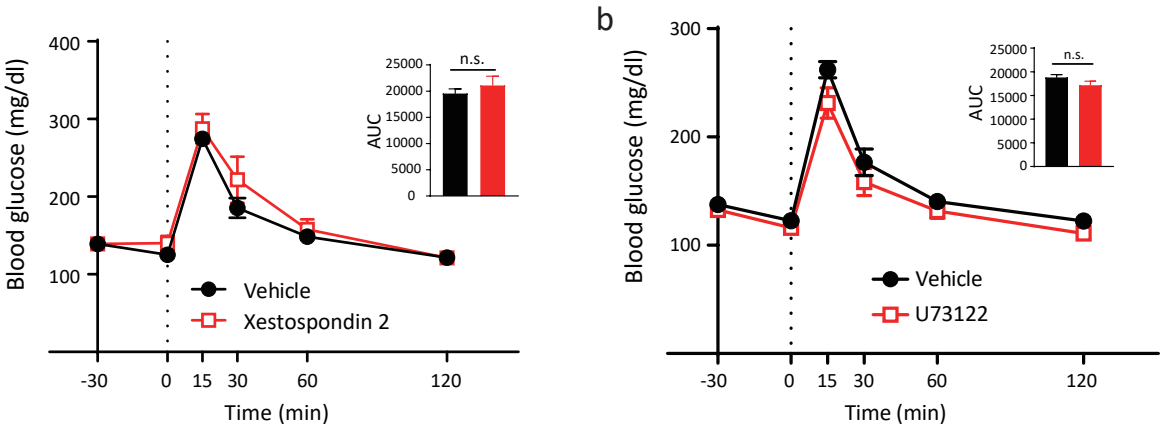

Figure 4. Hypothalamic PLC-mediated-pathway does not affect systemic glucose metabolism.

(a) Glucose tolerance test (GTT) (0–120 min) after intra-hypothalamic injection (-30 min) of Xestospondin, an IP3 receptor antagonist, (n=7) or vehicle (n=7). (b) GTT (0–120 min) after intra-hypothalamic injection (-30 min) of U73122, a phospholipase C (PLC) inhibitor, (n=7) or vehicle (n=7). All data represent the mean ± SEM

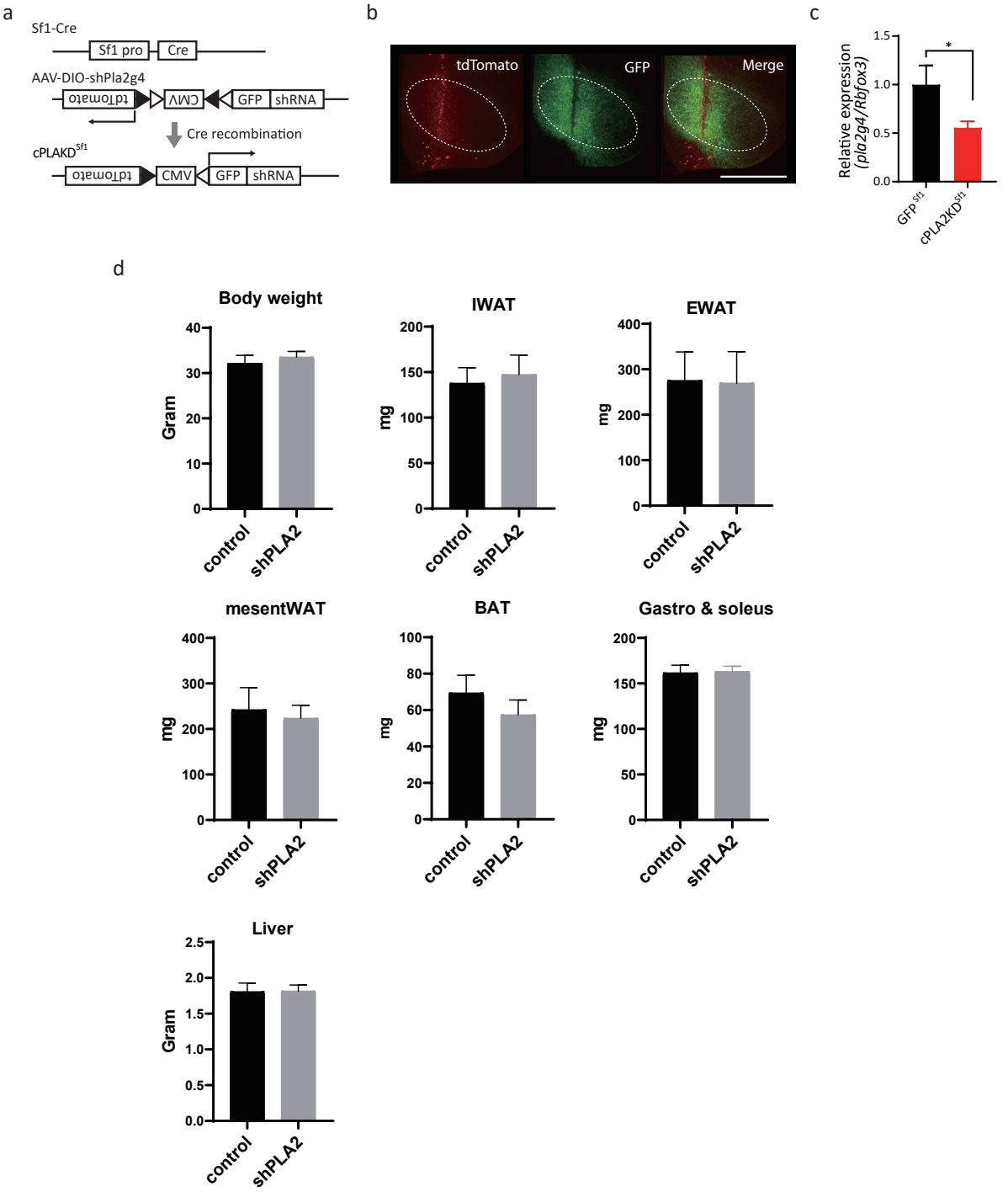

Figure 5. Knockdown of cPLA2 in Sf1 neurons does not affect body and tissue weight.
(a) Construct of AAV8-DIO (CreOn)-shRNA against *mpla2g4*, containing DIO (Double-floxed Inverted Open reading frame) to express shRNA Cre-dependently. (b) Representative micrographs showing virus infected (tdTomato) and shRNA expressing (GFP) Sf1-neurons. Scale bar: 500 μm. (c) Expression of *pla2g4a* mRNA in the whole hypothalamus injected with AAV8-DIO-shRNA against *mpla2g4* (cPLA2KD^{Sf1}; n=3) compared with control mice (GFP^{Sf1}; n=3). (d) Body weight and tissue weight in cPLA2KD^{Sf1} mice (n=5) and GFP^{Sf1} mice (n=5). (IWAT: inguinal white adipose tissue. EWAT: epididymal white adipose tissue. mesentWAT: mesenteric white adipose tissue. BAT: brown adipose tissue.)
All data represent the mean ± SEM

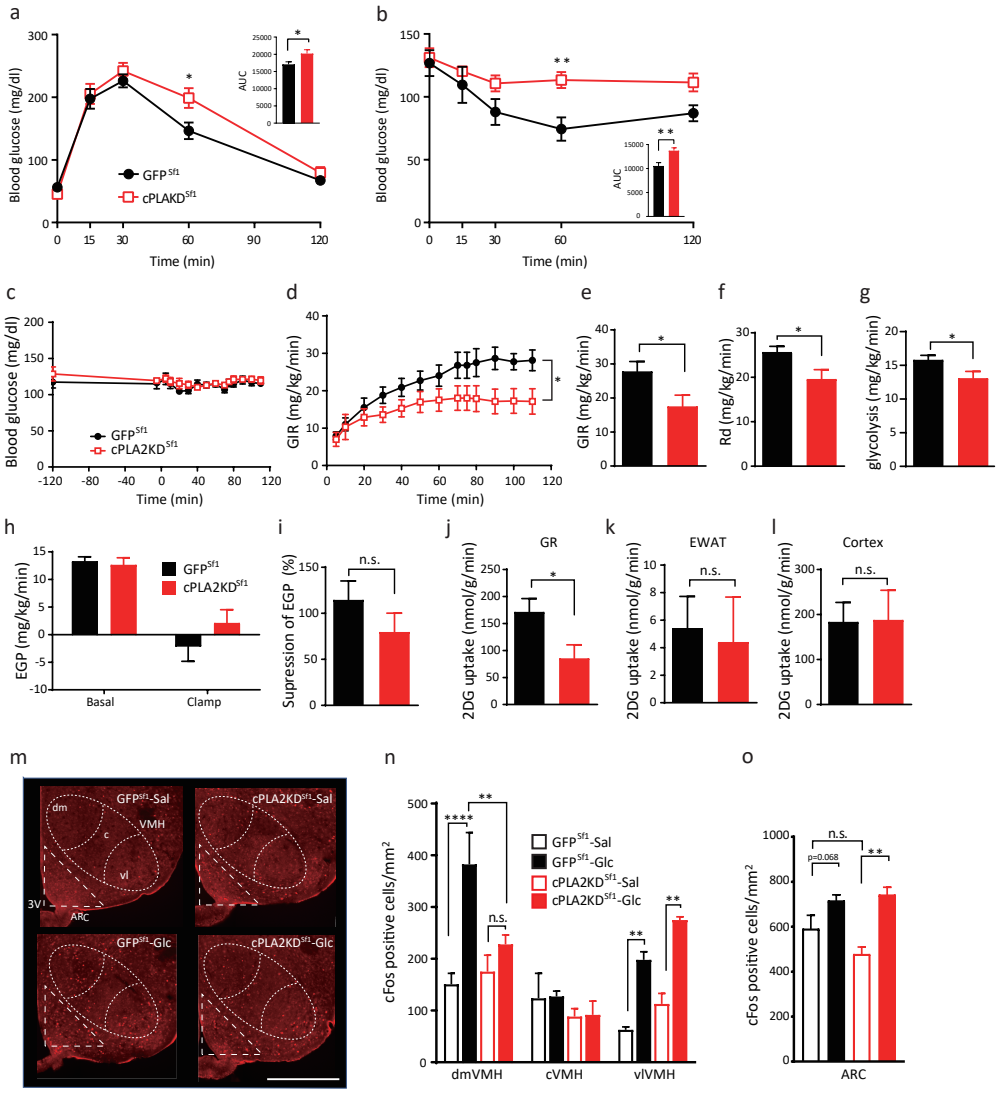

Figure 6. Knockdown of Sf1-neuronal *pla2g4a* impairs systemic glucose metabolism. (a) Glucose tolerance test in cPLA2KD ^{Sf1} (n=6) and GFP^{Sf1} mice (n=6). (b) Insulin tolerance test in cPLA2KD^{Sf1} (n=6) and GFP^{Sf1} mice (n=6). (C–L) Hyperinsulinemic–euglycemic clamp studies in cPLA2KD^{Sf1} and GFP^{Sf1} mice. (c) Blood glucose levels during hyperinsulinemic–euglycemic clamp studies in cPLA2KD^{Sf1} or GFP^{Sf1} mice. (d) The glucose infusion rate (GIR) required to maintain euglycemia during the clamp period in cPLA2KD^{Sf1} (n=7) or GFP^{Sf1} mice (n=7). (e) The average GIR between 75 and 115 min in cPLA2KD^{Sf1} (n=7) or GFP^{Sf1} mice (n=7). (f) The rate of glucose disappearance (Rd) during the clamp period, which represents whole-body glucose utilization. (g) The rates of whole-body glycolysis in cPLA2KD^{Sf1} (n=7) or GFP^{Sf1} mice (n=7). (h) Endogenous glucose production (EGP) during both the basal and clamp periods in cPLA2KD^{Sf1} (n=7) or GFP^{Sf1} (n=7). (i) Insulin-induced suppression of EGP in cPLA2KD^{Sf1} (n=7) or GFP^{Sf1} (n=7). (j–l) Graphs showing 2-[^{14}C]-Deoxy-D-Glucose uptake in red portions of the gastrocnemius (GR; j), white adipocyte (EWAT; k) and brain (cortex; l) during the clamp period in cPLA2KD^{Sf1} (n=7) or GFP^{Sf1} mice (n=7). (m) Representative micrographs showing immunofluorescent cFos staining in the hypothalamus of cPLA2KD^{Sf1} and GFP^{Sf1} mice after saline or glucose injection (3 g/kg). Scale bar: 500 µm. (n and o) Quantification of cFos expression in the dmVMH, cVMH, vlVMH and ARC of cPLA2KD^{Sf1} or GFP^{Sf1} mice after saline (n=3) or glucose (n=3) injection (3 g/kg). All data represent the mean ± SEM; * = p<0.05; ** = p<0.01; *** = p<0.001; **** = p<0.0001.

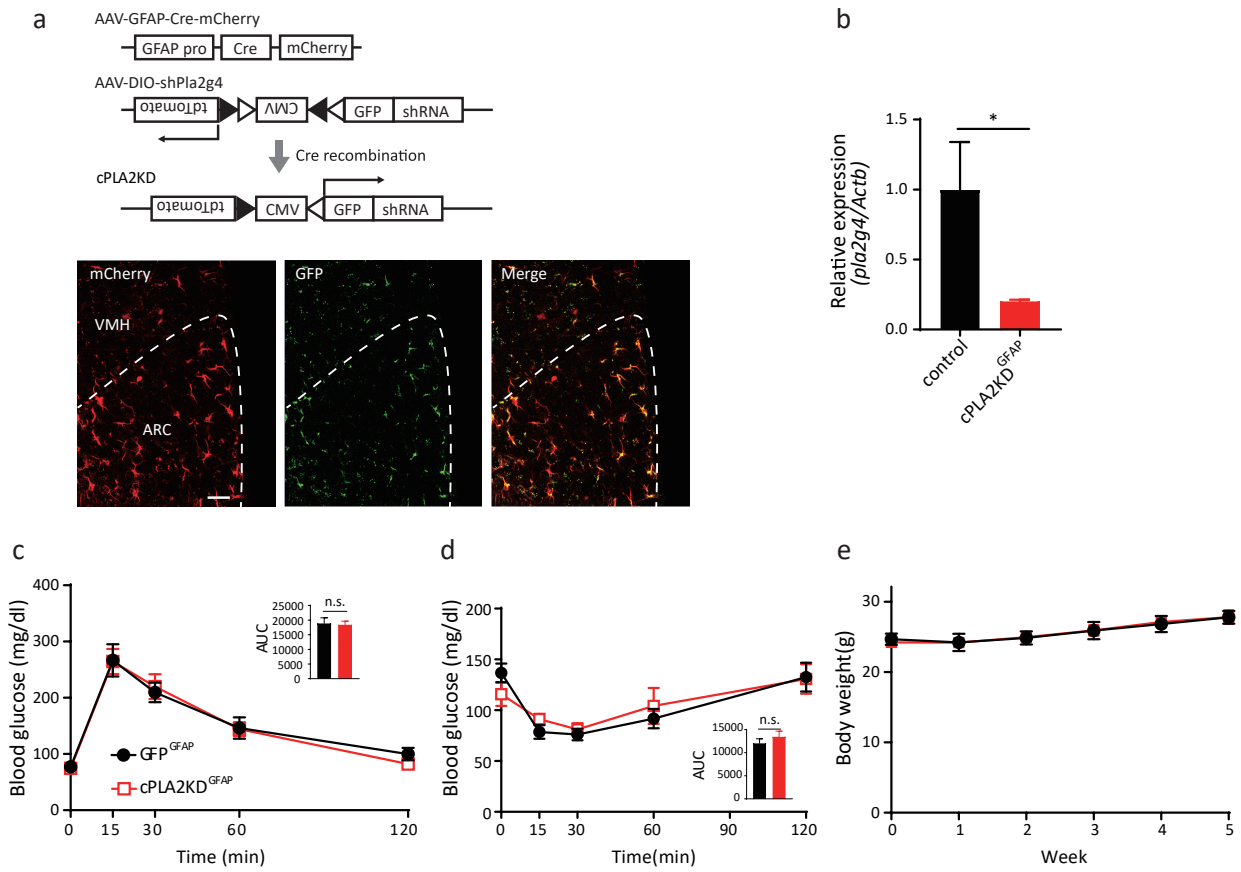

Figure 7. Knockdown of astrocytic cPLA2 in hypothalamus (cPLA2KD^{GFAP}) did not change body weight and glucose metabolism.
(a) Construct of AAV8-GFAP-Cre-mCherry and AAV8-DIO-shRNA against *mpla2g4* and representative micrographs showing virus infected (tdTomato) and shRNA expressing (GFP) astrocytes in the ARC. Scale bar: 25 μm. (b) Relative expression of cPLA2 in the hypothalamus of cPLA2KD^{GFAP} and control mice. n=3 in each experimental group. (c) Glucose tolerance test in cPLA2KD^{GFAP} mice (n=10) and GFP^{GFAP} mice (n=9). (d) Insulin tolerance test in cPLA2KD^{GFAP} mice (n=10) and GFP^{GFAP} mice (n=9). (e) Body weight change in cPLA2KD^{GFAP} mice (n=10) and GFP^{GFAP} mice (n=9) after viral injection. All data represent the mean ± SEM.

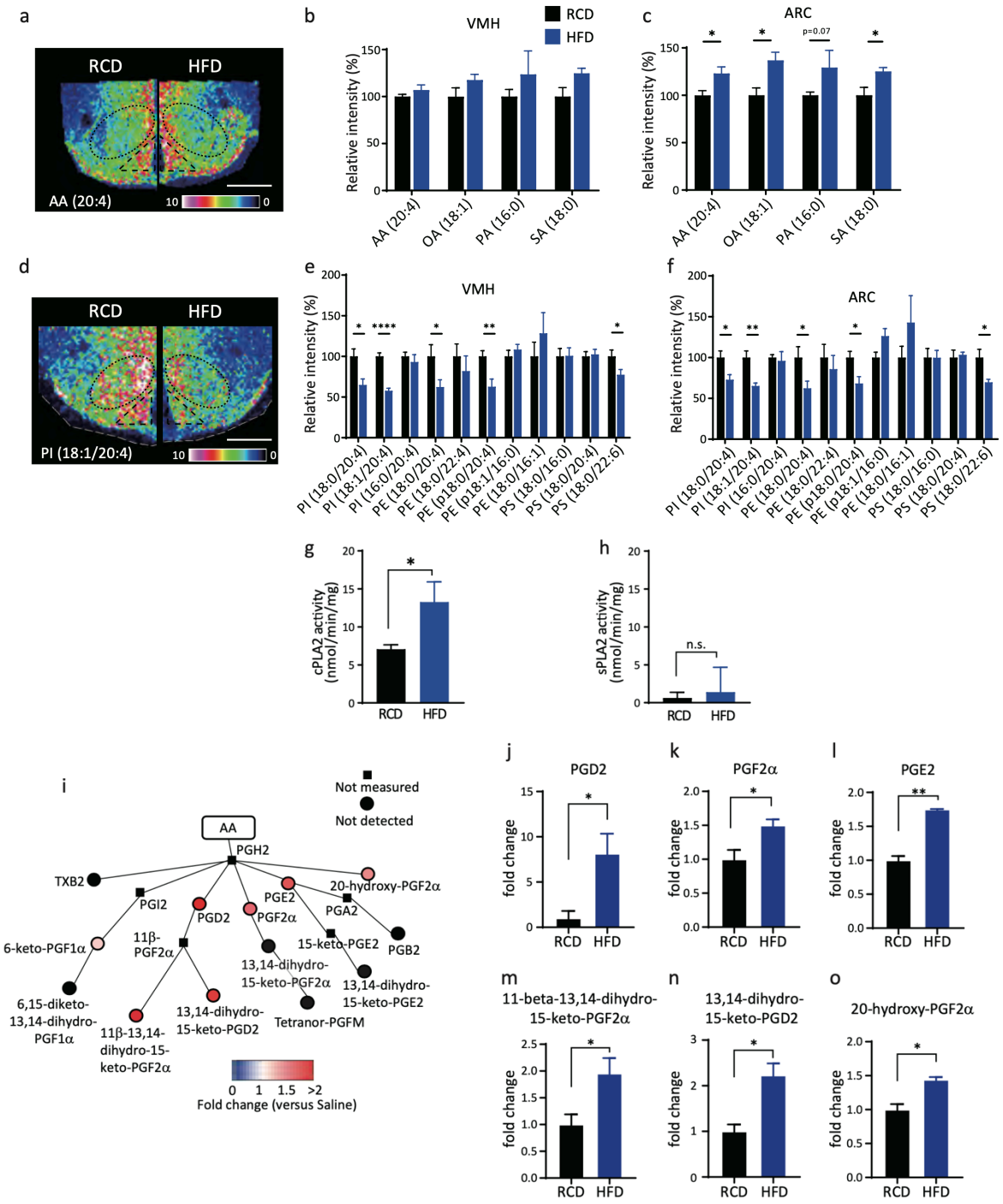

Figure 8. HFD feeding increases prostaglandin production derived from phospholipids. (a–f) Distributions of fatty acids and phospholipids in the hypothalamus in RCD- or HFD-fed mice for 8 weeks. (a and d) Representative results of IMS on hypothalamic arachidonic acid (AA) (a) and PI (18:1/20:4) (d) from RCD-fed mice (left) or HFD-fed mice (right). Scale bar: 500 μm. (b and c) Relative intensities of fatty acids in the VMH (b) or ARC (c) of RCD- (n=5) or HFD-fed mice (n=4). (e and f) Relative intensities of phospholipids in the VMH (e) or ARC (f) of RCD- (n=5) or HFD-fed (n=4) mice. (g and h) Enzymatic activity of hypothalamic cPLA2 (g) and sPLA (h) in RCD- (n=5) or HFD-fed (n=5) mice. (i) Relative amounts of prostaglandins in the hypothalamus after 8 weeks in HFD-fed mice (n=3) compared with those of RCD-fed mice (n=3). (j–o) Bar graphs showing COX-mediated production of (j) PGD2, (k) PGF2α, (l) PGE2, (m) 11-beta-13,14-dihydro-15-keto-PGF2α, (n) 13,14-dihydro-15-keto-PGD2 and (o) 20-hydroxy-PGF2α in 8 weeks of HFD-fed mice (n=3) compared with RCD-fed mice (n=3). All data represent the mean ± SEM; * = p<0.05; ** = p<0.01; *** = p<0.001; **** = p<0.0001.

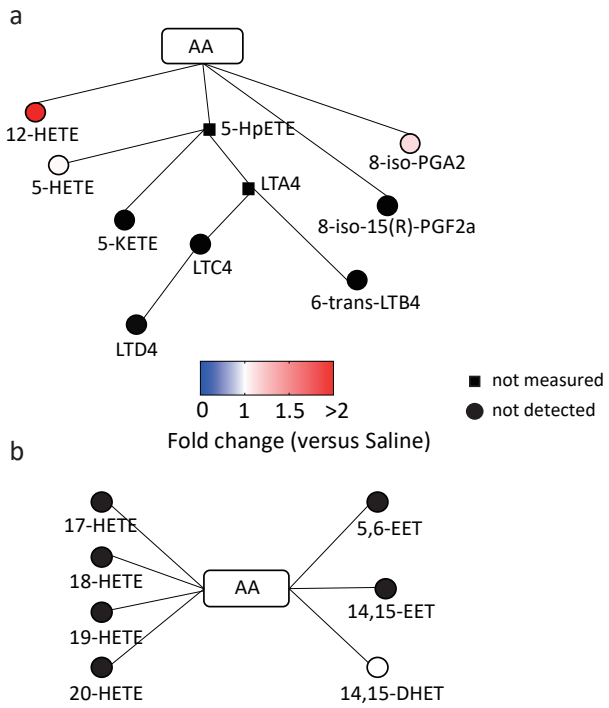

Figure 9. Effects of HFD on lipoxygenase or cytochrome P450 mediated eicosanoids in hypothalamus

Relative amounts of hypothalamic eicosanoids mediated by lipoxygenase (a) or cytochrome P450 (b) in RCD or HFD fed mice. n=3 each experimental group. Data represent the mean fold change in color.

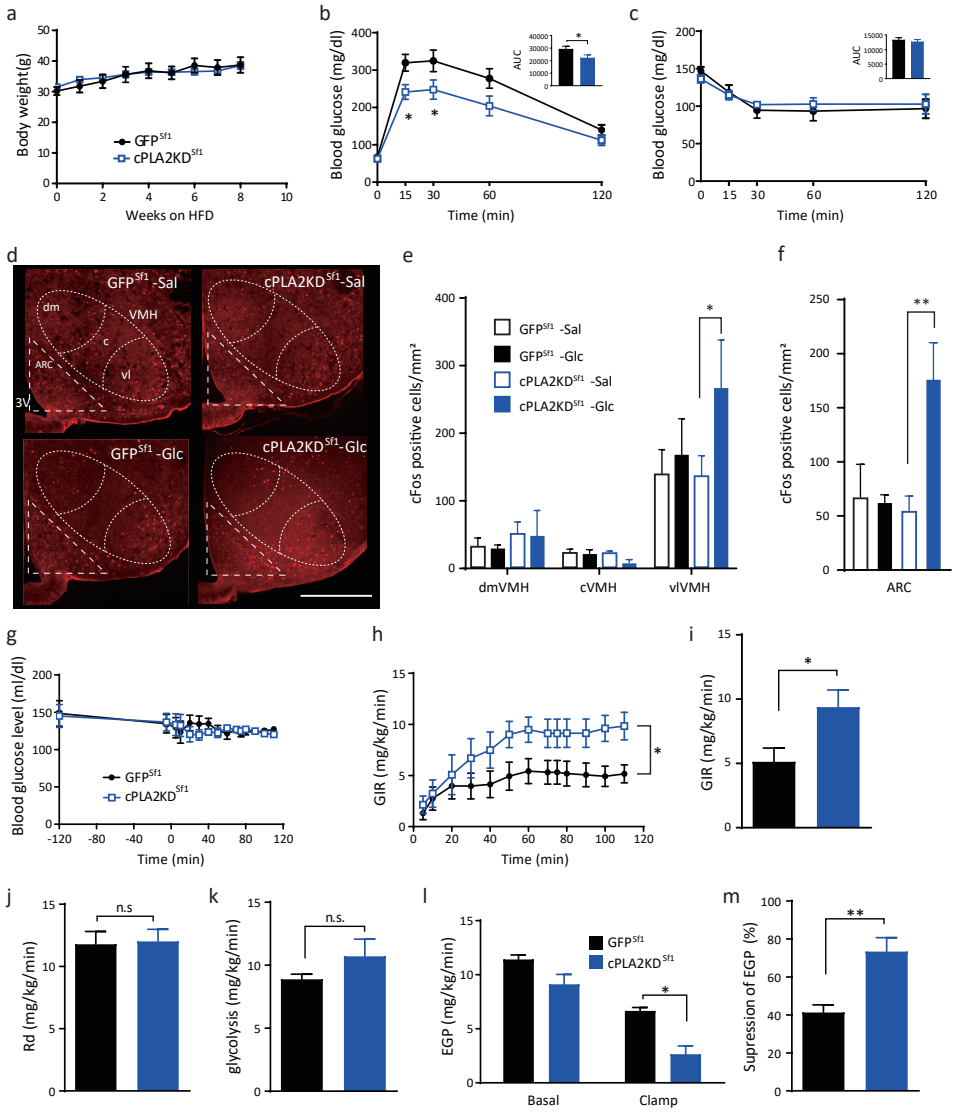

Figure 10. Knockdown of cPLA2 improves HFD-induced impairment of glucose metabolism.

(a) Body weight change in cPLA2KD^{Sfl} mice (n=12) and GFP^{Sfl} mice (n=10). (b) Glucose tolerance test on cPLA2KD^{Sfl} mice (n=12) and GFP^{Sfl} mice (n=10). (c) Insulin tolerance test on cPLA2KD^{Sfl} (n=8) mice and GFP^{Sfl} mice (n=6) during 8 weeks of HFD feeding. (d) Representative micrographs showing immunofluorescent cFos staining in the hypothalamus of HFD-fed cPLA2KD^{Sfl} and GFP^{Sfl} mice after saline or glucose injection. Scale bar: 500 μm. (e and f) Quantification of cFos expression in the dmVMH, cVMH, vlVMH (e), and ARC (f) of HFD-fed cPLA2KD^{Sfl} or GFP^{Sfl} mice after saline or glucose injection (n=3–5 in each experimental group). (g–m) Hyperinsulinemic–euglycemic clamp studies in HFD-fed cPLA2KD^{Sfl} (n=7) or GFP^{Sfl} (n=7) mice. (g) Blood glucose levels during hyperinsulinemic–euglycemic clamp studies in HFD-fed cPLA2KD^{Sfl} (n=7) or GFP^{Sfl} (n=7) mice. (h) The glucose infusion rate (GIR) required to maintain euglycemia during the clamp period in cPLA2KD^{Sfl} (n=7) or GFP^{Sfl} (n=7) mice. (i) The average GIR between 75 and 115 min in cPLA2KD^{Sfl} or GFP^{Sfl} mice. (j) The rate of glucose disappearance (Rd) during the clamp period, which represents whole body glucose utilization. (k) The rates of whole-body glycolysis in cPLA2KD^{Sfl} or GFP^{Sfl} mice. (l) Endogenous glucose production (EGP) during both basal and clamp periods in cPLA2KD^{Sfl} or GFP^{Sfl} mice. (m) The percent-suppression levels of EGP induced by insulin infusion in cPLA2KD^{Sfl} (n=7) or GFP^{Sfl} (n=7) mice. All data represent the mean ± SEM; * = $p<0.05$; ** = $p<0.01$.

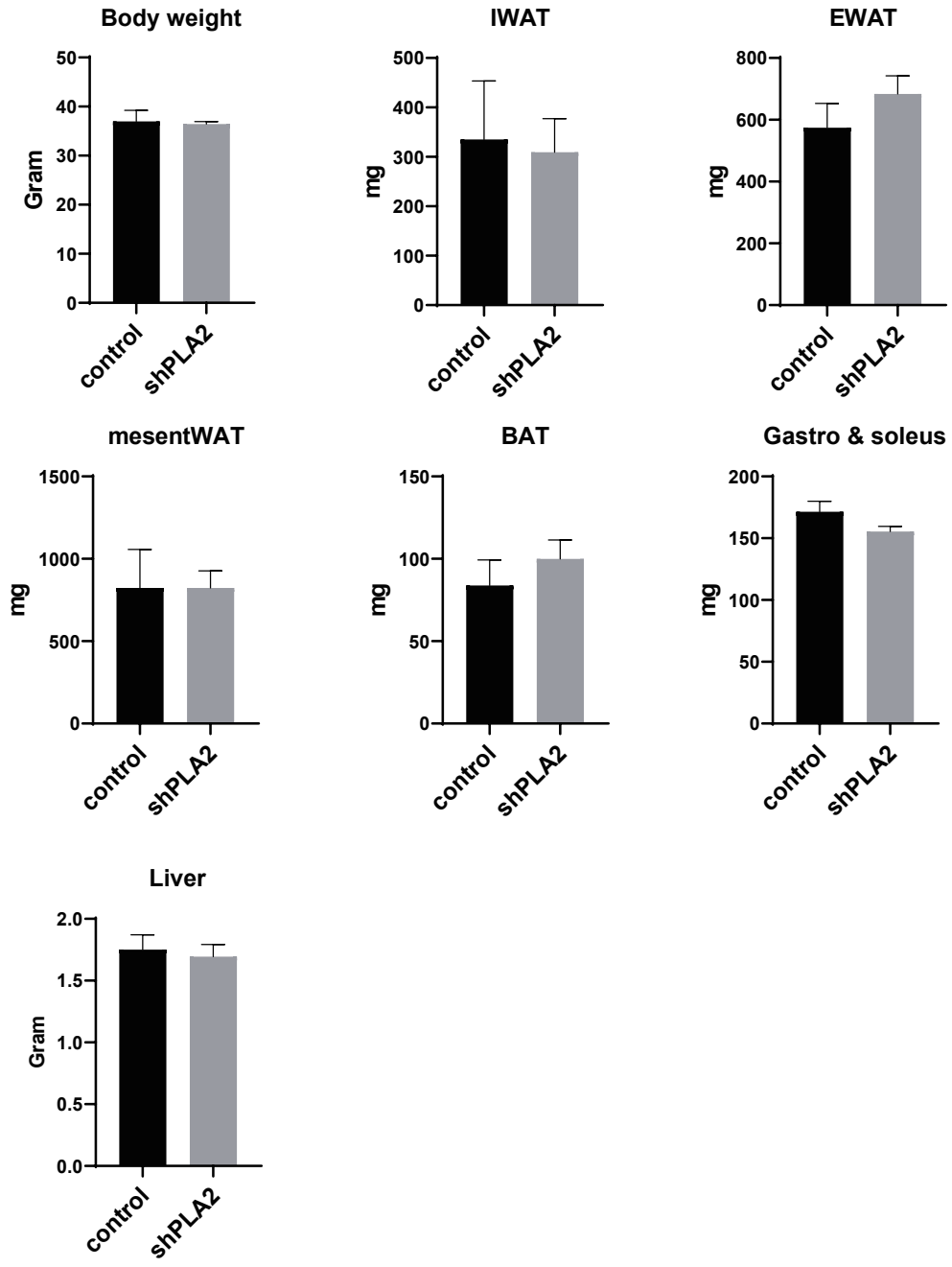

Figure 11. Knockdown of cPLA2 in Sf1 neurons does not affect body and tissue weight. Body weight and tissue weight in cPLA2KD^{Sf1} mice (n=5) and GFP^{Sf1} mice (n=5) after 8 weeks of HFD feeding. (IWAT: inguinal white adipose tissue. EWAT: epididymal white adipose tissue. mesentWAT: mesenteric white adipose tissue. BAT: brown adipose tissue.)

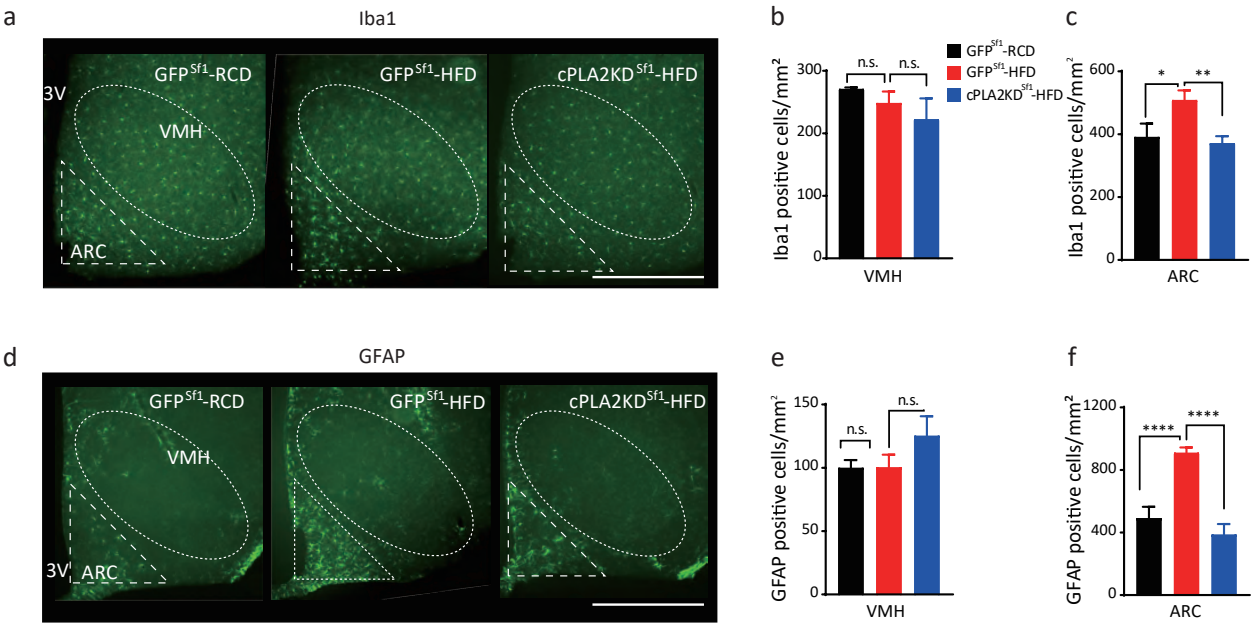

Figure 12. Knockdown of cPLA2 prevents HFD-induced microgliosis and astrogliosis.
(a) Representative micrographs showing immunofluorescent Iba1 staining in the hypothalamus of RCD-fed GFP^{Sfl} mice (GFP^{Sfl}-RCD), HFD-fed GFP^{Sfl} mice (GFP^{Sfl}-HFD) and HFD-fed cPLA2KD^{Sfl} (cPLA2KD^{Sfl}-HFD) mice. Scale bar: 500 µm. (b and c) Quantification of Iba1-positive cells in the VMH (b) or ARC (c) of GFP^{Sfl}-RCD (n=5), GFP^{Sfl}-HFD (n=8) and cPLA2KD^{Sfl}-HFD (n=5) mice. (d) Representative micrographs showing immunofluorescent GFAP staining in the hypothalamus of GFP^{Sfl}-RCD, GFP^{Sfl}-HFD and cPLA2KD^{Sfl}-HFD mice. Scale bar: 500 µm. (e and f) Quantification of GFAP-positive cells in the VMH (e) or ARC (f) of GFP^{Sfl}-RCD (n=5), GFP^{Sfl}-HFD (n=8) and cPLA2KD^{Sfl}-HFD (n=5) mice.
All data represent the mean ± SEM; * = $p<0.05$; ** = $p<0.01$; *** = $p<0.001$; **** = $p<0.0001$.

Table 1

Assignment to lipid molecular species by MS/MS negative ion mode.

Lipid assignment	$[M-H]^-$(*m/z*)
Palmitic acid	255.25
Oleic acid	281.3
Stearic acid	283.35
Arachidonic acid	303.3
DHA	327.33
PE (p18:1/16:0), plasmalogen	700.6
PE (18:0/16:1)	716.6
PE (p18:0/20:4), plasmalogen	750.5
PS (18:0/16:0)	762.6
PE (18:0/20:4)	766.5
PE (18:0/22:4)	794.5
PS (18:0/20:4)	810.6
PS (18:0/22:6)	834.6
PI (16:0/20:4)	857.6
PI (18:1/20:4)	883.55
PI (18:0/20:4)	885.77

Discussion

The roles of hypothalamic phospholipids and eicosanoids in the regulation of energy homeostasis is ill-defined. In this study, we found that the composition of phospholipids in the hypothalamus, especially AA attached phospholipids, are dynamically affected by blood glucose levels. cPLA2 in the VMH plays an important role in AA metabolism to produce prostaglandins and increase insulin sensitivity in muscle during hyperglycemia in RCD-fed mice. cPLA2-mediated phospholipid metabolism also regulates glucose-responsiveness in the dmVMH. HFD feeding, which promotes hyperglycemia, continuously activates cPLA2 and produces prostaglandins. The increased prostaglandins by HFD feeding could be a reason to induces inflammation in the hypothalamus and impairs glucose-sensing, by which attenuates insulin sensitivity in peripheral organs. Therefore, cPLA2-mediated phospholipid metabolism in the hypothalamus is critical for the physiological and pathological control of systemic glucose homeostasis.

FAs and PUFAs are believed to be transported from the bloodstream to the hypothalamus, and FA metabolism in the hypothalamus changes food intake and energy expenditure[24,35]. However, we observed reductions in AA-containing phospholipids and increases in prostaglandins in the hypothalamus after glucose injection. This suggests that AA is produced from intrinsic membrane phospholipids in the hypothalamus to make eicosanoids during hyperglycemia. Interestingly, the quantity of hypothalamic AA is not changed by hyperglycemia, suggesting production of prostaglandin from AA is increased to respond hyperglycemia. In line with this, inhibition of prostaglandin production by injecting COX inhibitor impaired glucose tolerance. It has been reported that FA oxidation by carnitine palmitoyltransferase I in the VMH plays important roles in food intake and energy homeostasis[36]. However, our data showed that the cPLA2 in Sf1 neurons has a minor effect on changes in body weight and tissue weight. This suggests that cPLA2 in Sf1 neurons controls glucose metabolism, but not body weight regulation, and it is likely that FAs generated from phospholipids are utilized for prostaglandin production.

AA exists in the sn-2 position of phospholipids, and cPLA2 is the rate-limiting enzyme for catalyzing AA by extracellular stimulation. cPLA2 is activated by an increase in the intracellular calcium concentration and by the phosphorylation of 505-serine residue, which is induced by the MAP kinase pathway[37]. The mechanism that activated cPLA2 in our study remains to be elucidated. However, we found that the glucose-induced activation of the dmVMH is dependent on prostaglandin production by Sf1 neurons. Sf1 neurons exist mainly in the dmVMH and cVMH, and most AA-containing phospholipids were found near the third ventricle in our study. Therefore, the hyperglycemia-induced prostaglandin production occurs in the medial part of the hypothalamus and affects neuronal activity in this region probably via changes in ion channel activities[38]. Similarly, prostaglandins regulate glucose-induced insulin secretion (GSIS) from pancreatic beta cells[39]. GSIS is the most studied mechanism of glucose-sensing. Thus, it is possible that a similar mechanism for prostaglandins affecting GSIS may be involved in the hypothalamic glucose sensing. Neurons in the vlVMH and ARC are also glucose sensing neurons[40,41]. In line with this, we showed increased c-Fos expression after glucose injection in healthy mice. However, the both regions remained glucose responsiveness after injection of cPLA2 inhibitor,

suggesting the prostaglandins play a minor role in glucose-sensing of vlVMH/ARC. interestingly, the vlVMH/ARC has different roles with dmVMH in regulating glucose metabolism: The vlVMH/ARC regulates glucose production in liver and the dmVMH controls glucose expenditure in skeletal muscle. These results corresponding with that chemoactivation of Sf1 neurons in dmVMH increases 2DG uptake rather than changes gluconeogenesis in liver[7].

Sf1 neurons are critical for the regulation of whole body energy homeostasis[7,42]. Activation of VMH neurons increases glucose uptake in skeletal muscle and BAT, but not in WAT or other organs[43,44]. Similar results were found in mice with intra-VMH administration of leptin[13,14,45]. Leptin receptors locate in the dmVMH and is required to maintain normal glucose homeostasis[8,46]. Approximately half of glucose-sensing neurons in the VMH respond to leptin[47]. Although the relationship between glucose-sensing and leptin remained blurred, glucose-sensing by Sf1 neurons via UCP2 is critical for systemic glucose metabolism[4], suggesting glucose-sensing neurons regulates glucose metabolism independent of leptin effects. Therefore, it is plausible that activation of the GE neurons in the dmVMH regulates insulin sensitivity in skeletal muscle through cPLA2-mediated prostaglandin production.

A HFD feeding causes diet-induced-obesity (DIO) and a state of chronic, low-grade inflammation occurs in several tissues, including the hypothalamus[20]. This hypothalamic inflammation is accompanied by an accumulation of microglia, and these changes decrease activities of POMC and AgRP neurons in response to several endocrine signals, such as leptin and insulin[48]. Additionally, a HFD feeding increases astrogliosis in the ARC, paraventrical hypothalamus and dorsomedial hypothalamus, but not the VMH[49]. Consistent with this, our data show that a HFD feeding induces microgliosis and astrogliosis in the ARC but not the VMH, which indicates that the VMH has different inflammatory responses to obesity[49]. After the mice in this study were fed with HFD, FAs such as AA, OA, PA and SA accumulated in the hypothalamus, especially in ARC. However, AA-containing phospholipids decreased because of an increase in hypothalamic cPLA2 activity. Prostaglandins are proinflammatory signals in the brain[50] and knockdown of cPLA2 in Sf1 neurons attenuates inflammation in the hypothalamus.

Our data suggest that the cPLA2-mediated production of prostaglandins in Sf1 neurons enhances inflammatory responses in the whole hypothalamus, including the ARC. Even though Sf1 neurons exist dmVMH, the prostaglandin production originated from the dmVMH may enhance inflammatory responses in the whole hypothalamus, including the ARC and vlVMH. Our results showed HFD feeding destroyed neuronal glucose-sensing in the vlVMH of control mice. This impairment of glucose-sensing in vlVMH was recovered in cPLA2KD^{sf1} mice accompany with ameliorated hypothalamic inflammation. Therefore, the cPLA2 may serve as a deteriorative role in the glucose-sensing of the vlVMH/ARC by inducing hypothalamic inflammation. It is likely that the long-term production of prostaglandins, which has a physiological role in glucose metabolism in RCD-fed mice, initiates HFD-induced inflammation and impairs glucose-sensing.

We also found that a HFD feeding abolished the increase in cFos expression induced by glucose in the VMH and ARC, which is consistent with the report that DIO decreases glucose sensing by VMH and

POMC neurons[21,41]. In HFD fed mice, the glucose-sensing of vlVMH and ARC were improved by knockdown of cPLA2. However, this improvement was not observed in the dmVMH, which senses glucose through cPLA2-dependent mechanism. This indicates that the attenuation of glucose sensing has already occurred in the dmVMH of HFD-fed mice by knockdown of cPLA2, thus the dmVMH of cPLA2KD^{sf1} mice could not respond to the glucose injection like vlVMH after HFD feeding.

Our data suggest that inflammation of the hypothalamus contributes to attenuating glucose sensing by the VMH and ARC. POMC and AgRP neurons are reported to regulate hepatic insulin sensitivity, but not muscle glucose metabolism[17,18,51]. Therefore, the improvement of the neuronal activity in the ARC contributes to restoring glucose metabolism by changing insulin sensitivity in the liver. Although knockdown of cPLA2 impaired glucose-sensing of dmVMH, it is supposed that knockdown of cPLA2 recovered part of neuronal functions in dmVMH by ameliorating hypothalamic inflammation.

Aspirin, a COX inhibitor, suppresses insulin sensitivity in healthy human[52–54], but improves insulin resistance in diabetic patients[55]. Our results were in a good agreement with the human studies. The hypothalamic prostaglandin production may be critical for the effects of aspirin on the whole body insulin sensitivity.

In summary, our study shows that the cPLA2 is fundamental for the function of the hypothalamus in regulating glucose homeostasis (Figure 13). In RCD fed mice, neuronal cPLA2 is necessary for glucose-sensing of dmVMH to control blood glucose levels. However, cPLA2 in the VMH has the critical role in inducing hypothalamic inflammation. Mice with knockdown of cPLA2 in Sf1 neurons resist diet-induced hypothalamic inflammation and keep the function vlVMH to respond to glucose. Therefore, the role of cPLA2-mediated eicosanoid production in the hypothalamus is different between RCD and HFD. Our findings provide novel evidence that cPLA2-mediated phospholipid metabolism in hypothalamic neurons plays an important role in systemic glucose metabolism.

Figure 13. Graphic abstract

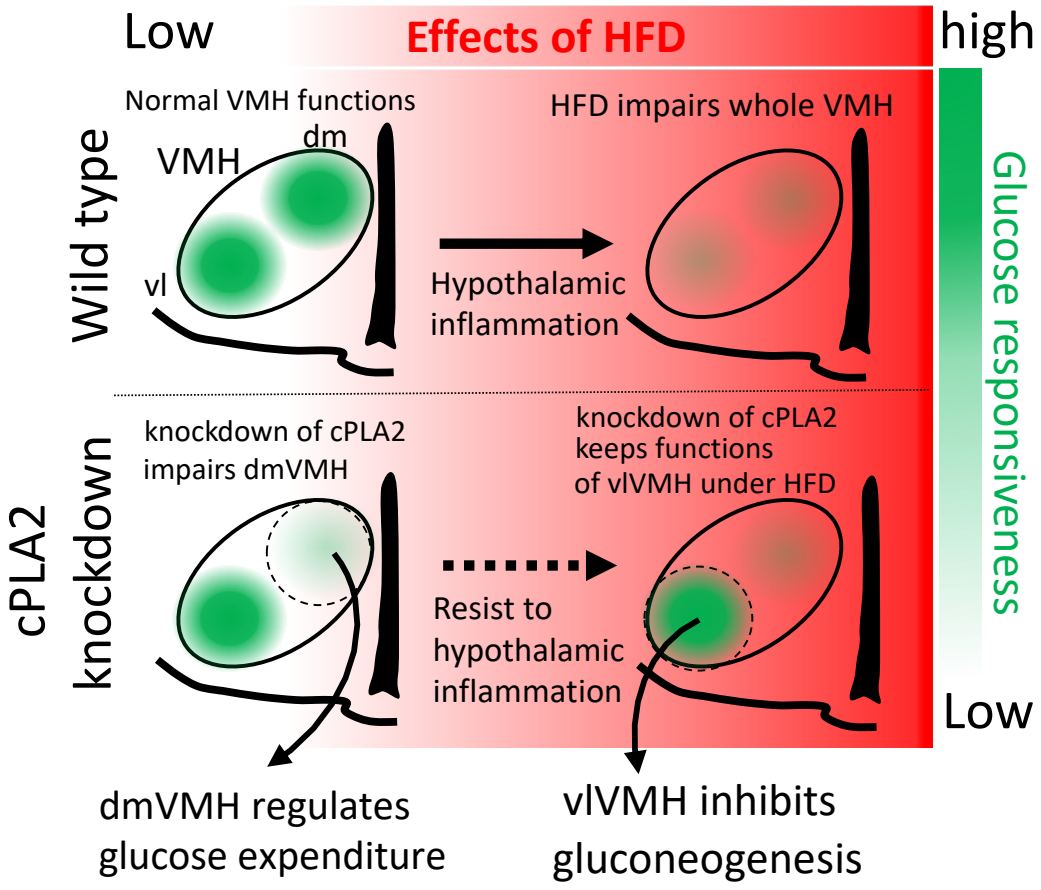

Conclusion

The hypothalamus is the central region to regulate physiological responses such as feeding, sleeping and thermal homeostasis. This region also plays a critical role in regulating glucose homeostasis by detecting blood glucose level and controls peripheral glucose utilization and hepatic glucose production. Obesity disturbs hypothalamus-regulated glucose homeostasis. Deciphering the mechanism of hypothalamic glucose-sensing and how obesity impairs glucose-sensing will provide new strategies to develop therapy for diabetes and obesity.

The brain is enriched with phospholipids containing poly-unsaturated fatty acids, which regulate several physiological responses by themselves or their metabolites including prostaglandins. However, the relationship between hypothalamic prostaglandins and systemic glucose metabolism is unclear. In addition, whether diet-induced obesity affects production of hypothalamic prostaglandins is also unknown. Therefore, this study aims to understand the role of hypothalamic prostaglandins in glucose-sensing by which regulates systemic glucose metabolism.

In this study, distribution of several phospholipids includes phosphatidyl-inositol (PI), phosphatidyl-ethanolamine (PE) phosphatidyl-serine (PS) in the hypothalamus was revealed by image mass spectrometry. Compared to saline injection, intraperitoneal glucose injection decreased amounts of PI (18:0/20:4), PI (18:1/20:4) and PE (18:0/20:4) in the hypothalamic ventromedial nucleus (VMH), and PI (18:0/20:4), PI (18:1/20:4), PE (18:0/20:4) and PS (18:0/16:0) in the arcuate nucleus (ARC). Most of these phospholipids contained a hydrophobic tail of arachidonic acid (AA), suggesting glucose injection may enhance AA releasing form the phospholipids. Liquid chromatography–mass spectrometry (LC-MS) revealed the amounts of metabolites of AA such as 6-keto-PGF1α, PGD2, 13,14-dihydro-15-keto-PGF2α and PGE2 increased after glucose injection.

Pharmacological inhibition of cytosolic phospholipase A2 (cPLA2), a key enzyme for generating AA from phospholipids, in the hypothalamus impaired systemic glucose metabolism and glucose-sensing of VMH. The same results were observed by inhibition of cyclooxygenase 1/2 (COX1/2), enzymes for prostaglandin production, suggesting the phospholipid-derived AA plays an important role in regulating hypothalamic glucose-sensing by increasing hypothalamic prostaglandins. In control mice, intraperitoneal glucose injection increased cFos expression in the VMH and ARC suggested the existence of glucose-sensing neurons. Inhibition of hypothalamic cPLA2 or COX1/2 abolished the glucose-induced cFos expression in the dorsomedial-VMH (dmVMH), suggesting the AA plays an important role in glucose-sensing.

To understand the role of phospholipid-derived AA specifically in the VMH, cPLA2 was knocked down in steroidogenic factor 1 neurons of the VMH by delivering short-hairpin RNA against *pla2g4a*. Knockdown of cPLA2 in the VMH during regular chow diet (RCD) feeding did not affect body weight and tissue weight. However, the knockdown mice had lower glucose tolerance and insulin sensitivity, which were consistent with the results by pharmacological inhibition of cPLA2 or COX1/2. Hyperinsulinemia-euglycemia clamp study showed this impairment was caused by decreased glucose utilization of skeletal muscle rather than hepatic glucose production. Glucose induced cFos expression

was abolished by knockdown of cPLA2 in the dmVMH. Therefore, the phospholipid-derived AA in the VMH regulated neuronal glucose-sensing.

The high fat diet (HFD) which impairs systemic glucose metabolism blunted glucose-sensing and abolished glucose-induced cFos expression in the VMH. The amounts of PI (18:0/20:4), PI (18:1/20:4), PE (18:0/20:4), PE (18:0/20:4) and PS (18:0/22:6) were decreased after 8 weeks of HFD feeding. The hypothalamic cPLA2 activity was higher in HFD fed mice than in RCD fed mice. Moreover, PGD2, PGF2α, PGE2, 11-beta-13,14-dihydro-15-213 keto-PGF2 α, 13,14-dihydro-15-keto-PGD2 and 20-hydroxy-PGF2 α also increased after HFD feeding, suggesting the production of prostaglandins from phospholipid-derived AA was increased.

The AA and prostaglandins are inflammatory factors. They accumulate in the hypothalamus in HFD fed mice and result in hypothalamic inflammation and impairment of neuronal functions. The increased AA and prostaglandins were caused by HFD induced overactivation of cPLA2, which agreed with the role of cPLA2 in inflammatory responses. Knockdown of cPLA2 in the VMH improved the down-regulation of hypothalamic glucose-sensing and glucose tolerance by HFD feeding. During HFD, the knockdown mice had recovered glucose-sensing in ventrolateral-VMH (vlVMH) rather than dmVMH. The impaired glucose-sensing of VMH was recovered in the vlVMH but not dmVMH because of a cPLA2 dependent pathway in dmVMH. Hyperinsulinemia-euglycemia clamp indicated the improved systemic glucose metabolism was caused by enhanced suppression of hepatic glucose production, which suggested the hepatic insulin sensitivity was increased. Further investigation of the role of cPLA2 in the HFD fed mice showed knockdown of cPLA2 ameliorates HFD-induced hypothalamic inflammation. Our data suggested that cPLA2-mediated phospholipid metabolism is critical for glucose-sensing of VMH by which controls systemic glucose metabolism during RCD. However, continuous activation of the same cPLA2-mediated pathway produces prostaglandins during HFD by which causes hypothalamic inflammation deteriorates glucose-sensing and systemic glucose metabolism. Moreover, we found that the dmVMH and vlVMH have different roles in regulating glucose-metabolism: the dmVMH regulates glucose utilization of skeletal muscle while the vlVMH control hepatic glucose production. This study reveals a new mechanism of diet-mediated metabolic disorders and will provide a direction for development of new therapy for diabetes.

Acknowledgements

First, I would like to express my sincere gratitude to my supervisor Professor Kazuhiro KIMURA who accepted me as a PhD student in this lab. Without his permission, I could not have the chance to finish this thesis and PhD degree. He always shows highly patient with me and teachs me how to be an independent researcher. He provided a lot of important comments on my thesis and made the thesis better. Professor KIMURA is strict on research including presentation and paper works, but he is also kind to treat student's problems. I admire him on his leadership and I'm trying to be a person like him.

I appreciate Assistant Professor Chitoku TODA who guided me on the research during these years. I very admire his knowledge and scientific sense. In research, he gave me a clear way toward our research goal which let me understand what I should do. On the other hand, he always encourages and supports me to do any research I want to do. This is the important point for me to be an independent researcher. The experience of working with him increases my enthusiasm in scientific research very much and makes me confident to take more challenges.

I also thank Associated Professor Yuko OKAMATSU-OGURA who always wears smile on her face and is friendly to everyone. In meeting or discussion, she usually commented on presentations of my research with some points we ignored. Without her critical comments I could not be able to make high quality research.

I also want to express my thankfulness to Dr. Izumi YAMAMOTO. She is always positive on experimental results and propose many interesting points on research. Moreover, she usually shows her kind consideration when I was frustrated. She is my best friend in Japan.

I thank my dissertation committee members Professor Kenichi OTSUGURO and Professor Osamu INANAMI for their advice on dissertation.

I would like to thank all lab members in Laboratory of Biochemistry for their kind treatments on me. Thank them for translating things from Japanese to English. I might have problems and might not finish the PhD course without their kind helps.

Finally, I have to present my best appreciation to my parents and my wife. Without their support, I could not confront so many challenges during these years.

References

1. Pozo M and Claret M. Hypothalamic Control of Systemic Glucose Homeostasis: The Pancreas Connection. Trends Endocrinol Metab 29, 581–594, 2018.
2. Ruud J, Steculorum SM, and Brüning JC. Neuronal control of peripheral insulin sensitivity and glucose metabolism. Nat Commun 8, 15259, 2017.
3. Hetherington AW and Ranson SW. The relation of various hypothalamic lesions to adiposity in the rat. J Comp Neurol 76, 475–499 ,1942.
4. Toda C, Kim JD, Impellizzeri D, Cuzzocrea S, Liu ZW, and Diano S. UCP2 Regulates Mitochondrial Fission and Ventromedial Nucleus Control of Glucose Responsiveness. Cell 164, 872–883, 2016.
5. Kunwar PS, Zelikowsky M, Remedios R, Cai H, Yilmaz M, Meister M, and Anderson DJ. Ventromedial hypothalamic neurons control a defensive emotion state. eLife 4, e06633, 2015.
6. Meek TH, Nelson JT, Matsen ME, Dorfman MD, Guyenet SJ, Damian V, Allison MB, Scarlett JM, Nguyen HT, Thaler JP, Olson DP, Myers MG Jr, Schwartz MW, and Morton GJ. Functional identification of a neurocircuit regulating blood glucose. PNAS 113, E2073–E2082 ,2016.
7. Coutinho EA, Okamoto S, Ishikawa AW, Yokota S, Wada N, Hirabayashi T, Saito K, Sato T, Takagi K, Wang CC, Kobayashi K, Ogawa Y, Shioda S, Yoshimura Y, and Minokoshi Y. Activation of SF1 Neurons in the Ventromedial Hypothalamus by DREADD Technology Increases Insulin Sensitivity in Peripheral Tissues. Diabetes 66, 2372–2386, 2017.
8. Sohn JW, Oh Y, Kim KW, Lee S, Williams KW, and Elmquist JK. Leptin and insulin engage specific PI3K subunits in hypothalamic SF1 neurons. Mol Metab 5, 669–679, 2016.
9. Klöckener T, Hess S, Belgardt BF, Paeger L, Verhagen LA, Husch A, Sohn JW, Hampel B, Dhillon H, Zigman JM, Lowell BB, Williams KW, Elmquist JK, Horvath TL, Kloppenburg P, and Brüning JC. High-fat feeding promotes obesity via insulin receptor/PI3K-dependent inhibition of SF-1 VMH neurons. Nat Neurosci 14, 911–918, 2011.
10. Roberts CK, Hevener AL, and Barnard RJ. Metabolic Syndrome and Insulin Resistance: Underlying Causes and Modification by Exercise Training. Compr Physiol 3, 1–58, 2013.

11. Park HK and Ahima RS. Physiology of leptin: energy homeostasis, neuroendocrine function and metabolism. Metabolism 64, 24–34, 2015.
12. Minokoshi Y, Haque MS, and Shimazu T. Microinjection of leptin into the ventromedial hypothalamus increases glucose uptake in peripheral tissues in rats. Diabetes 48, 287–291, 1999.
13. Toda C, Shiuchi T, Lee S, Yamato-Esaki M, Fujino Y, Suzuki A, Okamoto S, and Minokoshi Y. Distinct effects of leptin and a melanocortin receptor agonist injected into medial hypothalamic nuclei on glucose uptake in peripheral tissues. Diabetes 58, 2757–2765, 2009.
14. Toda C, Shiuchi T, Kageyama H, Okamoto S, Coutinho EA, Sato T, Okamatsu-Ogura Y, Yokota S, Takagi K, Tang L, Saito K, Shioda S, and Minokoshi Y. Extracellular Signal–Regulated Kinase in the Ventromedial Hypothalamus Mediates Leptin-Induced Glucose Uptake in Red-Type Skeletal Muscle. Diabetes 62, 2295–2307, 2013.
15. Barsh GS and Schwartz MW. Genetic approaches to studying energy balance: perception and integration. Nat Rev Genet 3, 589–600, 2002.
16. Roh E and Kim MS. Brain Regulation of Energy Metabolism. Endocrinol Metab (Seoul) 31, 519–524, 2016.
17. Dodd GT, Michael NJ, Lee-Young RS, Mangiafico SP, Pryor JT, Munder AC, Simonds SE, Brüning JC, Zhang ZY, Cowley MA, Andrikopoulos S, Horvath TL, Spanswick D, and Tiganis T. Insulin regulates POMC neuronal plasticity to control glucose metabolism. eLife 7, e38704, 2018.
18. Könner AC, Janoschek R, Plum L, Jordan SD, Rother E, Ma X, Xu C, Enriori P, Hampel B, Barsh GS, Kahn CR, Cowley MA, Ashcroft FM, and Brüning JC. Insulin Action in AgRP-Expressing Neurons Is Required for Suppression of Hepatic Glucose Production. Cell Metab 5, 438–449, 2007.
19. Routh VH, Hao L, Santiago AM, Sheng Z, and Zhou C. Hypothalamic glucose sensing: making ends meet. Front Syst Neurosci 8, 2014.
20. Cai D and Khor S. “Hypothalamic Microinflammation” Paradigm in Aging and Metabolic Diseases. Cell Metab 30, 19–35, 2019.
21. Stoelzel CR, Zhang Y, and Cincotta AH. Circadian-timed dopamine agonist treatment reverses high-fat diet-induced diabetogenic shift in ventromedial hypothalamic glucose sensing. Endocrinol Diab Metab 3, 2020.
22. Loftus TM, Jaworsky DE, Frehywot GL, Townsend CA, Ronnett GV, Lane MD, and Kuhajda FP. Reduced Food Intake and Body Weight in Mice Treated with Fatty Acid Synthase Inhibitors. Science 288, 2379–2381, 2000.

23. Pocai A, Obici S, Schwartz GJ, and Rossetti LA. brain-liver circuit regulates glucose homeostasis. Cell Metab 1, 53–61, 2005.
24. Bazinet RP and Layé S. Polyunsaturated fatty acids and their metabolites in brain function and disease. Nat Rev Neurosci 15, 771–785, 2014.
25. Ghosh M, Tucker DE, Burchett SA, and Leslie CC. Properties of the Group IV phospholipase A2 family. Prog Lipid Res 45, 487–510, 2006.
26. Nonogaki K, Iguchi A, Yatomi A, Uemura K, Miura H, Tamagawa T, Ishiguro T, and Sakamoto N. Dissociation of hyperthermic and hyperglycemic effects of central prostaglandin F2α. Prostaglandins 41, 451–462, 1991.
27. Migrenne S, Cruciani-Guglielmacci C, Kang L, Wang R, Rouch C, Lefèvre AL, Ktorza A, Routh VH, Levin BE, and Magnan C. Fatty Acid Signaling in the Hypothalamus and the Neural Control of Insulin Secretion. Diabetes 55, S139–S144, 2006.
28. Obici S, Feng Z, Morgan K, Stein D, Karkanias G, and Rossetti L. Central administration of oleic acid inhibits glucose production and food intake. Diabetes 51, 271–275, 2002.
29. Kita H, Kochi S, Imai Y, Yamada A, and Yamaguchi T. Rigid external distraction using skeletal anchorage to cleft maxilla united with alveolar bone grafting. Cleft Palate Craniofac J 42, 318–327, 2005.
30. Yamada M, Kita Y, Kohira T, Yoshida K, Hamano F, Tokuoka SM, and Shimizu T. A comprehensive quantification method for eicosanoids and related compounds by using liquid chromatography/mass spectrometry with high speed continuous ionization polarity switching. J Chromatogr B 995–996, 74–84, 2015.
31. Ayala JE, Bracy DP, McGuinness OP, and Wasserman DH. Considerations in the design of hyperinsulinemic-euglycemic clamps in the conscious mouse. Diabetes 55, 390–397, 2006.
32. Farooqui AA, Yang HC, Rosenberger TA, and Horrocks LA. Phospholipase A2 and Its Role in Brain Tissue. J Neurochem 69, 889–901, 1997.
33. Macedo F, dos Santos LS, Glezer I, and da Cunha FM. Brain Innate Immune Response in Diet-Induced Obesity as a Paradigm for Metabolic Influence on Inflammatory Signaling. Front Neurosci 13, 2019.
34. Posey KA, Clegg DJ, Printz RL, Byun J, Morton GJ, Vivekanandan-Giri A, Pennathur S, Baskin DG, Heinecke JW, Woods SC, Schwartz MW, and Niswender KD. Hypothalamic proinflammatory lipid accumulation, inflammation, and insulin resistance in rats fed a high-fat diet. Am J Physiol Endocrinol Metab 296, E1003–E1012, 2009.
35. Rapoport SI, Chang MC, and Spector AA. Delivery and turnover of plasma-derived essential PUFAs in mammalian brain. J Lipid Res 42, 678–685, 2001.

36. Bruce KD, Zsombok A, and Eckel RH. Lipid Processing in the Brain: A Key Regulator of Systemic Metabolism. Front Endocrinol (Lausanne) 8, 2017.
37. Lin LL, Wartmann M, Lin AY, Knopf JL, Seth A, and Davis RJ. cPLA2 is phosphorylated and activated by MAP kinase. Cell 72, 269–278, 1993.
38. Jang Y, Kim M, and Hwang SW. Molecular mechanisms underlying the actions of arachidonic acid-derived prostaglandins on peripheral nociception. J Neuroinflammation 17, 2020.
39. Carboneau BA, Breyer RM, and Gannon M. Regulation of pancreatic β-cell function and mass dynamics by prostaglandin signaling. J Cell Commun Signal 11, 105–116, 2017.
40. He Y, Xu P, Wang C, Xia Y, Yu M, Yang Y, Yu K, Cai X, Qu N, Saito K, Wang J, Hyseni I, Robertson M, Piyarathna B, Gao M, Khan SA, Liu F, Chen R, Coarfa C, Zhao Z, Tong Q, Sun Z, and Xu Y. Estrogen receptor-α expressing neurons in the ventrolateral VMH regulate glucose balance. Nat Commun 11, 2020.
41. Parton LE, Ye CP, Coppari R, Enriori PJ, Choi B, Zhang CY, Xu C, Vianna CR, Balthasar N, Lee CE, Elmquist JK, Cowley MA, and Lowell BB. Glucose sensing by POMC neurons regulates glucose homeostasis and is impaired in obesity. Nature 449, 228–232, 2007.
42. Shimazu T and Minokoshi Y. Systemic Glucoregulation by Glucose-Sensing Neurons in the Ventromedial Hypothalamic Nucleus (VMH). J Endocr Soc 1, 449–459, 2017.
43. Shimazu T, Sudo M, Minokoshi Y, and Takahashi A. Role of the hypothalamus in insulin-independent glucose uptake in peripheral tissues. Brain Res Bull 27, 501–504, 1991.
44. Sudo M, Minokoshi Y, and Shimazu T Ventromedial hypothalamic stimulation enhances peripheral glucose uptake in anesthetized rats. Am J Physiol.261, E298-303, 1991.
45. Kamohara S, Burcelin R, Halaas JL, Friedman JM, and Charron MJ. Acute stimulation of glucose metabolism in mice by leptin treatment. Nature 389, 374–377, 1997.
46. Dhillon H, Zigman JM, Ye C, Lee CE, McGovern RA, Tang V, Kenny CD, Christiansen LM, White RD, Edelstein EA, Coppari R, Balthasar N, Cowley MA, Chua S Jr, Elmquist JK, and Lowell BB. Leptin Directly Activates SF1 Neurons in the VMH, and This Action by Leptin Is Required for Normal Body-Weight Homeostasis. Neuron 49, 191–203, 2006.
47. Irani, BG, Le Foll C, Dunn-Meynell A, and Levin BE. Effects of leptin on rat ventromedial hypothalamic neurons. Endocrinology 149, 5146–5154, 2008.
48. Zhang R, Dhillon H, Yin H, Yoshimura A, Lowell BB, Maratos-Flier E, and Flier JS. Selective Inactivation of Socs3 in SF1 Neurons Improves Glucose Homeostasis without Affecting Body Weight. Endocrinology 149, 5654–5661, 2008.

49. Buckman LB, Thompson MM, Moreno HN, and Ellacott KLJ. Regional astrogliosis in the mouse hypothalamus in response to obesity. J Comp Neurol 521, 1322–1333, 2013.
50. Palumbo S and Bosetti F. Alterations of brain eicosanoid synthetic pathway in multiple sclerosis and in animal models of demyelination: Role of cyclooxygenase-2. Prostaglandins, Leukot Essent Fat Acids 89, 273–278, 2013.
51. Berglund ED, Vianna CR, Donato J Jr, Kim MH, Chuang JC, Lee CE, Lauzon DA, Lin P, Brule LJ, Scott MM, Coppari R, and Elmquist JK. Direct leptin action on POMC neurons regulates glucose homeostasis and hepatic insulin sensitivity in mice. J Clin Invest 122, 1000–1009, 2012.
52. Bratusch-Marrain PR, Vierhapper H, Komjati M, and Waldhäusl WK. Acetyl-salicylic acid impairs insulin-mediated glucose utilization and reduces insulin clearance in healthy and non-insulin-dependent diabetic man. Diabetologia 28, 671–676, 1985.
53. Giugliano D, Sacca L, Scognamiglio G, Ungaro B, and Torella R. Influence of acetylsalicylic acid on glucose turnover in normal man. Diabete Metab 8, 279–282, 1982.
54. Newman WP and Brodows RG. Aspirin causes tissue insensitivity to insulin in normal man. J Clin Endocrinol Metab 57, 1102–1106, 1983.
55. Hundal RS, Petersen KF, Mayerson AB, Randhawa PS, Inzucchi S, Shoelson SE, and Shulman GI. Mechanism by which high-dose aspirin improves glucose metabolism in type 2 diabetes. J Clin Invest 109, 1321–1326, 2002.

日本語要旨

視床下部は食欲、睡眠、体温維持など、動物にとって生命の維持に重要な生理現象の調節に関わる脳部位である。視床下部は血糖値の調節にも重要であり、血糖値の増減を感知することで、その状況に応じて末梢組織の糖利用または肝臓からの糖産生を調節して血糖値を一定に保つ。肥満はこの血糖値の恒常性維持機構の作用を抑制し、血糖値が正常に保てなくなる。どのようなメカニズムで脳が血糖値を感知するか、また、肥満が血糖値の感知を低下するかを解明することは糖尿病治療法の作成や新たな治療薬の開発に役立つ。

脳内には不飽和脂肪酸が細胞膜リン脂質の構成因子として存在し、様々な刺激によって遊離され、プロスタグランジン類の原料として利用される。しかし、血糖値の変化が視床下部のプロスタグランジン類を生成するか、また、視床下部のプロスタグランジン生成が血糖値の調節に重要であるかは不明である。さらに肥満における視床下部のプロスタグランジンの役割も分かっていない。本研究は、血糖値の変化や肥満が視床下部のプロスタグランジン類の生成にどのような影響を与えるか、また、生成されたプロスタグランジン類が全身糖代謝にどのような役割を持つかを明らかにすることを目的とする。

最初に、マウスの腹腔内にグルコースを投与し、視床下部の細胞膜リン脂質、特に Phosphatidyl-inositol (PI), Phosphatidyl-ethanolamine (PE)および Phosphatidyl-serine (PS)をイメージング質量分析器によって測定した。グルコースを投与すると、視床下部腹内側核および弓状核において PI (18:0/20:4)、PI (18:1/20:4)および PE (18:0/20:4)が生理食塩水群と比べて有意に低下し、アラキドン酸（20:4）が選択的に遊離していることが示唆された。そこで視床下部の全種類のエイコサノイドを高速液体クロマトグラフィー質量分析器（LC-MS）で調べると、グルコースの投与は 6-keto-PGF1α、PGD2 および PGE2 を増加させた。アラキドン酸は細胞膜リン脂質の sn-2 位に結合しており、これを加水分解する酵素は Phospholipase A2 (PLA2)である。そして、アラキドン酸からプロスタグランジンを生成する酵素は Cyclooxygenase 1/2 (COX1/2)である。マウスの視床下部に PLA2 または COX1/2 に対する阻害剤を投与し、グルコース負荷試験を行うと両方の阻害剤投与群は溶媒投与群よりも血糖値が増加した。従って、血糖値の増加は視床下部において PLA2 を活性化し、細胞膜リン脂質からアラキドン酸を遊離させ、プロスタグランジン類を生成することで血糖値を低下させることが示唆された。

神経細胞で重要であることが知られる細胞質型 PLA2 (cPLA2)の作用を調べるために、cPLA2 に対する shRNA を Cre-recombinase (Cre)の作用で発現するアデノ随伴ウイルスを作成した。腹内側核の神経特異的に Cre を発現する Steroidogenic factor 1 (Sf1-Cre)マウスを購入し、視床下部内にアデノ随伴ウイルスを投与することで腹内側核の神経特異的 cPLA2 ノックダウンマウス（$cPLA2KD^{Sf1}$）を作成した。$cPLA2KD^{Sf1}$ マウスはコントロールマウス(GFP^{Sf1})と比べて体重や成長に差はなかった。しかし、$cPLA2KD^{Sf1}$ マウスは GFP^{Sf1} よりもグルコース負荷試験、インスリン負荷試験および Hyperinsulinemic euglycemic clamp 試験において、骨格筋のインスリン

感受性および糖取り込みが低下していた。従って、腹内側核神経の cPLA2 は骨格筋の糖代謝に重要な役割を持つことが示唆された。

グルコースを投与すると神経活動の指標となる cFos で染色される細胞が腹内側核および弓状核で増加する。すなわち、視床下部には血糖値の増加を感知して活性化する細胞が存在する。PLA2 阻害剤、COX1/2 阻害剤または cPLA2 の shRNA を視床下部に作用させると、グルコースによる cFos の増加が腹内側核でのみ抑制された。従って、視床下部のプロスタグランジン類の生成は腹内側核による血糖値の感知に重要であることが示唆された。

次に、肥満を誘導する脂肪含量の高い餌（高脂肪食）を 8 週間マウスに与え、肥満における視床下部プロスタグランジン類の生成を調べた。高脂肪食飼育群は通常食群よりも弓状核におけるアラキドン酸、オレイン酸またはステアリン酸の含有量が優位に増加した。一方で、高脂肪食で飼育したにも関わらず、腹内側核および弓状核において PI (18:0/20:4)などのアラキドン酸含有リン脂質が通常食群よりも低下した。また、高脂肪食飼育群の視床下部において PGD2 などのプロスタグランジン類が通常食群よりも増加した。従って、高脂肪食によって肥満した場合も視床下部で細胞膜リン脂質からプロスタグランジン類が生成されることが示唆された。

肥満における視床下部 cPLA2 の役割を調べるために、cPLA2KD^{Sfl} マウスおよび GFP^{Sfl} マウスを高脂肪食で飼育した。cPLA2KD^{Sfl} マウスは GFP^{Sfl} マウスと比べて体重および脂肪組織重量には差はなかった。しかし、cPLA2KD^{Sfl} マウスは GFP^{Sfl} マウスよりも肝臓のインスリン感受性が亢進した。高脂肪食で飼育するとグルコース投与は視床下部で cFos を増加しなくなる。高脂肪食で飼育した cPLA2KD^{Sfl} マウスでは腹内側核の腹外側部および弓状核でグルコース投与による cFos の増加が回復した。GFP^{Sfl} マウスでは高脂肪食飼育によって腹内側核および弓状核のミクログリアのサイズが大きくなり、炎症反応を起こしていることが示唆された。しかし、cPLA2KD^{Sfl} マウスでは高脂肪食によるミクログリアの活性化は起こらなかった。従って、食事誘導性肥満は cPLA2 を介して視床下部のプロスタグランジン生成を増加し炎症を誘導すること、そして視床下部による血糖値感知機構を低下させ、肝臓のインスリン感受性を低下することが示唆された。

以上の研究により、マウスにおいて視床下部のプロスタグランジン生成は食事によって異なる作用を持つことが明らかとなった。通常食で飼育している時、視床下部のプロスタグランジン類は血糖値の感知に必要であり、骨格筋のインスリン感受性を増加する。一方で、高脂肪食で飼育している時は、視床下部のプロスタグランジン生成によって炎症が引き起こされ、視床下部による血糖値の感知が低下して、肝臓のインスリン感受性を低下する。本研究の結果は、全身糖代謝に重要な役割を持つ視床下部のプロスタグランジン類が、高脂肪食によって長期間作用するとむしろ糖尿病の悪化因子として働くことを示唆しており、適切な時期でプロスタグランジン生成の阻害剤を投薬することが糖尿病の治療に役立つ可能性を示している。今後、さらに研究を進め、新たな糖尿病治療方法の創出に貢献することが期待される。